TEMPERATURE RESPONSE OF WATER BODY WITH THERMAL EFFLUENT DISPOSAL

by

AJAY KUMAR AGRAWAL

DEPARTMENT OF MECHANICAL ENGINEERING

INDIAN INSTITUTE OF TECHNOLOGY KANPUR

JULY, 1982

TEMPERATURE RESPONSE OF WATER BODY WITH THERMAL EFFLUENT DISPOSAL

A Thesis Submitted
in Partial Fulfilment of the Requirements
for the Degree of

MASTER OF TECHNOLOGY

by

AJAY KUMAR AGRAWAL

to the

DEPARTMENT OF MECHANICAL ENGINEERING
INDIAN INSTITUTE OF TECHNOLOGY KANPUR

JULY, 1982

CERTIFICATE

This is to certify that the thesis entitled "Temperature Response of Water-body with Thermal Effluent Disposal" by Ajay Kumar Agrawal is a record of work carried out under my supervision and has not been submitted elsewhere for a degree.

July 1982

(Manohar Prasad)
Assistant Professor
Department of Mechanical Engineering
Indian Institute of Technology, Kanpur

ACKNOWLEDGEMENTS

I express my deep sense of gratitude to Dr. Manohar Prasad for his valuable guidance and critical appraisal throughout the work. Constant inspiration and encouragement provided by him led to the completion of this work.

Thanks are due to Mr. P.N. Sharma and Mr. P.N. Misra for their assistance in installing the experimental set-up.

Thanks are due to all my friends for making the stay at I.I.T. Kanpur a pleasant and memorable experience.

Special thanks are due to Mr. D.P. Saini for his patience during the typing of the manuscripts.

Ajay Kumar Agrawal

CONTENTS

LIST OF FIGURES

NOMENCLATURE

a	:	Constant used in Eq. 3.2.4
b	:	Constant used in Eq. 3.2.4
c_p	:	Specific heat
d_o	:	Jet diameter
E	:	Saturated vapor pressure
E_a	:	Partial vapor pressure of air
E_T	:	As defined by eq. 3.3.6
Fr	:	Froude number
Fr'	:	Densimetric Froude number
g	:	Gravitational acceleration
g'	:	Reduced gravitational acceleration
H	:	Depth of pond
$h(W)$	:	Mass-transfer coefficient
IP	:	Pool fraction
I	:	Number of depth element from the surface of water body
J	:	Number of time element
K	:	Overall surface heat-transfer coefficient
K_b	:	Back-radiation heat-transfer coefficient
K_c	:	Convection heat-transfer coefficient
K_e	:	Evaporation heat-transfer coefficient
k	:	Thermal conductivity of water
L	:	Enthalpy of evaporation
L_T	:	As defined by eq. 3.3.7

$\dot{m}$	:	Hot water flow rate
N	:	Number of depth elements
p	:	Number of iteration
Q	:	Net heat flux across air water interface
Q_a	:	Long wave atmospheric radiations absorbed by water
Q_b	:	Heat loss due to back radiations
Q_c	:	Heat loss due to convection
Q_e	:	Heat loss due to evaporation
Q_G	:	Short wave radiations absorbed by water
Q_T	:	As defined by eq. 3.3.2
QP	:	Plant heat load
Re	:	Reynolds number
T	:	Temperature
T_a	:	Air temperature
T_B	:	Base temperature
T_e	:	Equilibrium temperature
T_i	:	Discharge water temperature
T_n	:	Natural water temperature
T_O	:	Intake temperature
$\bar{T}_O$	:	Dimensionless intake temperature
ΔT	:	Excess temperature
ΔT_i	:	Temperature rise at discharge point
t	:	Time
V	:	Jet velocity
W	:	Wind velocity, km/h

Z : Co-ordinate

Z_s : Depth of buoyant pool.

Greek Symbols

β : Parameter used in Eq. 3.2.2

ϕ : Relative humidity

ε_Z : Eddy diffusivity

ν : Kinematic viscosity

ρ : Density

$\Delta\rho$: $(\rho_i - \rho_w)$

ρ_i : Density of hot water

ρ_w : Density of ambient water

σ : Stefan-voltzman constant

τ : Dimensionless time

Subscripts

m : Model

p : Prototype

r : Ratio of model to prototype

SYNOPSIS

TEMPERATURE RESPONSE OF WATER BODY WITH THERMAL EFFLUENT DISPOSAL

A Thesis Submitted
In Partial Fulfilment of the Requirements
For the Degree of

MASTER OF TECHNOLOGY

by

AJAY KUMAR AGRAWAL

to the

Department of Mechanical Engineering
Indian Institute of Technology, Kanpur
July 1982

To predict behavior of prototype systems, the range of operating variables for experiments is selected using a similitude criteria. Effects of intake location, discharge water flow rate and temperature rise are studied for water bodies of various depths. A bottom intake is the best choice because the buoyancy as well as mixing dominate in the upper zone only. Vertical as well as horizontal stratification occur during transient regime. At steady state an isothermal buoyant pool is established. It's depth

is characterized by a non-dimensional pool fraction which, in turn, depends upon the discharge conditions and intake location

Using a heat-balance and corresponding differential equations, transient distribution of natural and excess temperature in the water body are obtained. Overall heat-transfer coefficient at the water surface gives a quick guess of the temperature rise at given plant head load and weather conditions. Natural water temperature and wind velocity are the most influential factors for the determination of the excess temperature.

CHAPTER - 1

INTRODUCTION

1.1 DESCRIPTION:

The growing dependency upon electricity for scientific developments, industrial growth and prosperity of people has called for augmenting the power generation facilities. Todate, thermal power plants are the major source of electrical energy because of their low initial cost and short gestation period. The efficiency of such power plants depends upon the temperatures of heat source and sink. While the former is decided by the metallurgical limit the latter, in turn, is controlled by the choice of waste heat disposal system. Out of about 3 MW of energy transfer from the source to the heat engine for a typical power plant, nearly 2 MW is rejected to the sink, rendering about 1 MW of electrical power output. Therefore, water quantity on the order of 40 to 60 litres/s-MW of power generation, passes through the condenser, and generally gets heated up by 8-12°C, depending upon the system design. Waste heat is then dissipated to the earth's atmosphere through the use of cooling systems, that is river, lake, cooling pond, cooling tower, etc.

In once-through cooling systems, water is taken from a natural basin, and discharged into another part of it, where it is diffused by water currents and subsequently dissipated to atmosphere. This situation is favourable only for medium and small capacity thermal power plants located near sea, river or canal. The condenser cooling water is taken upstream and hot water discharged downstream resulting in elevated river temperature. It brings about ecological disturbances in larger distances. Therefore,the public regulatory measures of thermal pollution in river, canal etc. may forbid the discharge of hot water from power plants.

To overcome these limitations, the most common practice is the use of closed systems for cooling the condenser water. A few available systems are cooling towers, cooling ponds, natural reservoirs like lakes etc. In cooling towers, heat disposal is accomplished mainly by evaporation of water induced by enhanced air-water contact area. In cooling ponds/reservoirs (water bodies), the hot water is discharged at the surface and cool water withdrawn from the lower level. The plant heat is dissipated due to increased evaporation, convection and radiation at the air-water interface.

Because of high initial and operating costs compared to other closed systems, cooling towers are adopted only for zones of expensive land. Hence factors determining

power plant location invisage the utilization of naturally available cooling reservoirs till they are exhausted. Such systems require minimum operating and initial costs, rendering beneficial results in the long run. Despite involvement of additional initial investments, cooling ponds are exploited in absence of availability of natural reservoirs.

Cooling systems employing combinations of once-through system, cooling pond/reservoir and cooling tower have important influence on optimization among economics of power generation, environmental measures and energy conservation aspects. Adequate knowledge of behaviour of various mixed modes of operation require an exhaustive study of individual systems.

The study of cooling water bodies becomes momentous in view of their wide spread applicability in single as well as mixed mode operation of cooling systems. In the choice of a natural lake or design of a cooling pond, a major consideration is to increase the utilization factor of the basin to provide maximum cooling of water and possibility to cool water to the steady value of relatively low temperatures. In an ideal case, water should reach the natural water temperature which, in turn, is governed by meteorological and climatological factors of the geographical region, and unaffected by warm effluents from the plant. But, in practice

a temperature at intake higher than the natural water temperature is established. This excess temperature, the governing factor of power plant efficiency, can be minimized with the knowledge of temperature developments in the water bodies subjected to thermal discharge under various plant load conditions. Cooling efficiency of the system can be enhanced by directing the water currents in the cooling water body, to ensure maximum utilization of the temperature gradients and available surface area.

To avoid any short-circuiting of warm water, locations of intake and discharge points are important. For the investigation of behavior of cooling water bodies of various depths and configurations, plant variables (that is cooling water flow rate, water inlet temperature) and meteorological variables (that is ambient temperature, relative humidity and wind speed etc.) should be considered. To study the ecological aspects of the problem, prediction of excess temperature distribution established due to plant heat load and meteorological changes is required.

1.2 LITERATURE REVIEW:

Different aspects of the problem of heated discharge into water bodies have been investigated by several past researchers. These include the study of heat and mass transfer mechanisms at air-water interface, temperature

response of water bodies subjected to hot water discharge, and jet behavior under various discharge conditions. Experimental and analytical techniques have been presented for specific cases as reviewed below.

Raphael [1] developed a procedure including empirical relations for predicting the temperatures in water bodies. The heat and mass transfer coefficients were obtained from observed data on lakes. Edinger et al [2] have used equilibrium temperature method for the calculation of daily average heat-exchange. Since, equilibrium temperature, (temperature when net heat flux across the air-water interface is zero) may vary as much as 40°C in a day,its use as base temperature in linearizing the heat flux equation, is doubtful, and may be erroneous.

Ryan et al [3] developed a technique for accounting the contribution of free convection to the evaporation from a cooling pond and putforth its correlations with forced evaporation. The variation in the temperature difference encountered in practice is not large. Hence the temperature dependent term for natural convection, leading to complicated expression of heat-flux, can be substituted by a constant term.

Yotsukura et al [4] approximated the basic exchange equations for air-water interface by Taylor series

expansion around an undefined base temperature. Error analyses were done for linear and quadratic approximations. It was suggested that for most practical cases, a linear approximation gives acceptable solution. Jobson, H.E.[5] used natural water temperature for calculating a surface heat transfer coefficient, which, in turn, could be used to predict unnatural excess temperature. Kothandaraman, V.[6] presented a report upon an investigation regarding nature of seasonal and non-seasonal variations in the daily mean river temperature at a given location, and using Fourier Series analysis developed a method to predict natural water temperature on the basis of meteorological data.

Experiments on turbulent water jets discharged into a water body were first conducted by Jen et al [7] for various jet orientations discharging vertically, horizontally and at several angles in between, for different Froude numbers. The limitation to the use of results arises as the Orifice was located nearby at the bottom, which is seldom the case. Tamai, et al [8] have determined the mixing effects of warm water discharge, indicating therein a principal role of densimetric Froude number, being played in surface spreading of warm water.

A number of mathematical models, [9, 10, 11, 12] right from complicated three-dimensional to simplified

isothermal models have been found for prediction of temperature distribution in water bodies with space and time. Moore et al [9] have developed a simple model, based on perturbation technique, for thermal structure of a stratified lake. It considers various changes in equilibrium temperature and diffusion coefficient to represent heat addition and mixing effects of power plants on the thermal cycle of the lake. Surface heat exchange coefficient used is based on equilibrium temperature method, and its values have been taken constant for winter and summer periods. Mc Guirk, J.J. et al [10] have described finite difference calculations of three-dimensional heated surface jets discharging into stagnant water. The method presents the solution of continuity, lateral and longitudinal momentum and energy equations. Computed results compare well with experimental data. Similar approaches have been adopted by other workers [11, 12]. Most elaborate mathematical studies have been presented by Lee, S. et al [12]. They developed a time-dependent, three-dimensional, free surface numerical model with horizontal and vertical stretching. The effects of variable bottom topography, free surface elevations, surface heat transfer currents and meteorological conditions were considered. It provides sufficient three-dimensional information for study of water bodies.

Nystrom et al [13] conducted a number of physical model studies, field surveys and analyses. They have emphasized the necessity of similarity analysis between model and prototype studies. Froude, Reynold and densimetric Froude numbers formed a criteria for similarity analyses.

Recently the study of cooling ponds has received due attention. Jirka et al [14] presented an analysis of thermal stratification of cooling ponds and categorized using a non-dimensional pond number, the thermal structure of ponds into either the well stratified or partially mixed or vertically mixed type. Only long term mean thermal structure could be predicted. Therefore, any short-term variations due to meteorological changes or plant operating conditions cause transient deviations from the mean structure. Jirka et al [15] have considered the efficiency of various cooling ponds and concluded that deep stratified water bodies are most suitable configuration. Otherwise, for shallow cooling ponds, a moderate length/width ratio on the order of about 5-10 as well as some amount of baffling arrangement is recommended.

1.3 PRESENT STUDY:

It comprises experimental and analytical study of temperature developments in cooling water bodies having hot water discharge. Using similitude criteria, the operating

variables for experiments are selected with a view to predict behavior of prototype systems. Effects of plant operating conditions (that is, condenser water flow rate and its temperature rise), intake position, pond depth and wind velocity on transient and steady-state intake temperatures are studied extensively. At steady state, an isothermal layer is established in the upper zone because of turbulent mixing and buoyancy. Effects of discharge conditions and intake location on the depth of buoyant pool are investigated.

An energy balance equation is found for steady-state heat-exchange across the water surface. Mass-transfer coefficient, which is a function of wind velocity, is evaluated experimentally. A methodology is presented to calculate the excess temperature at water surface (ΔT), induced by thermal discharge. Meteorological variables, such as solar radiation, air-temperature, wind velocity, relative humidity etc. influence the thermal structure of water body. Therefore, the steady state analysis has been extended to obtain the transient variations of ΔT. An overall surface heat-transfer coefficient, comprising coefficients of convection, evaporation and back radiation heat-transfer, is used to predict ΔT. Differential equations for natural and excess temperature distribution in the water body are obtained and solved numerically.

CHAPTER-2

EXPERIMENTAL STUDY

2.1 THERMAL DISCHARGE INTO WATER BODY:

Various physical phenomena control the hydrodynamics of a heated effluent being transported from the outfall to the main receiving water body. In near field region, the effluent momentum and buoyancy govern the discharge trajectory and dilution. In intermediate region,buoyancy force become dominant and control plume spreading and depth. However, in the far field region, heat and mass-transfer at the air-water interface control the stratification characteristics.

The relative action of momentum and buoyancy forces along jet trajectory is measured by a local densimetric Froude number (Fr') :

$$Fr' = V / (\sqrt{g'Z'}) \qquad (2.1.1)$$

where,

V = horizontal velocity (m/s)

$g' = (\Delta\rho / \rho_i) \cdot g$ = reduced gravitational acceleration (m/s^2)

$\Delta\rho = (\rho_i - \rho_w)$

ρ_i = density of hot water (kg/m^3)

ρ_w = density of ambient water (kg/m^3)

Z = depth of water body (m)

Figure 2-1 exhibits the structure of a buoyant surface jet. At near field region, high values of velocity (V and reduced gravitational acceleration render Fr' >> 1, since ($\Delta\rho / \rho_i$) is nearly between 0.002 - 0.005 giving g'Z << 1. Momentum causes linear growth of jet, both laterally and vertically, and entrainment of surrounding fluid into turbulent jet region.

At larger distances Fr' decreases as V and g' decrease asymtotically. Therefore buoyancy exerts an increasing influence on the jet behavior, and starts dominating the inertial forces. Finally it causes an unsteady motion in all directions, rendering a gradual increase in length, width and thickness of the pool of buoyant water. After a long period of time a steady state, based on a balance between heat-loss to the atmosphere and heat addition through the discharge, results in the establishment of a buoyant pool in all the regions.

2.2 SIMILITUDE CRITERIA:

The study of prototype is, in general, extremely complex. Therefore it is a usual practice to simulate the prototype system using a model. The governing dimensionless numbers are sought to establish similarity. In the present

type of problem, model and prototype Froude number (Fr) should be equal. It represents the ratio of inertia force to gravity force, that is,

$$Fr = V / (\sqrt{g\ Z}) \qquad (2.2.1)$$

for similitude

$$Fr_m = Fr_p \qquad (2.2.2)$$

where subscripts 'm' and 'p' are used for model and prototype, respectively.

From Eqs. (2.2.1 and 2.2.2) with respective quantities one gets :

$$V_r = \sqrt{Z_r} \qquad (2.2.3)$$

having $V_r = V_m / V_p$ and $Z_r = Z_m / Z_p$

For kinematic similarity Reynold number 'Re' ($= V\ Z / \nu$, where ν is kinematic viscosity) which measures the relative action of inertia to viscous force, is used. It governs the flow pattern and mixing process. Therefore,

$$Re_r = Re_m / Re_p = V_r\ Z_r / \nu_r \qquad (2.2.4)$$

Since ν_r is unity, using Eq. (2.2.3), Re_m can be expressed as :

$$Re_m = Re_p\ (Z_r)^{3/2} \qquad (2.2.5)$$

Prototype Reynolds numbers are well within turbulent regime. Therefore, the value of model Reynolds number depends upon depth ratio. A minimum limit to the value of Re_m is imposed (500-1000) such that the model operates in turbulent regime [15]. This subsequently sets a lower limit on Z_r.

To achieve similitude of buoyancy, the densimetric Froude number must be equal in model and prototype. Therefore,

$$Fr'_r = V_r / \left(\sqrt{(\Delta\rho / \rho_i)_r \cdot g_r \cdot Z_r} \right) = 1 \qquad (2.2.6)$$

Using Eq. (2.2.3) into Eq. (2.2.6) with $g_r = 1$, one gets :

$$(\Delta\rho / \rho_i)_r = 1 \qquad (2.2.7)$$

Eq. (2.2.7) can be satisfied only if temperatures in model and prototype are the same. It implies, therefore, that for equal temperature rise at inlet, temperature profiles for model and prototype become similar. Therefore, the model study would enable the prediction of temperatures in prototype systems.

2.3 EXPERIMENTAL SET-UP

It consists of a water tank with various measuring and control devices for investigation of temperature developments and prediction of important design parameters. The arrangements for the study of effects of wind velocity and location of inlet and discharge points have also been

made. The overall set-up encompasses broader flexibility to facilitate the experimental study at desired conditions.

A schematic diagram of the system is shown in Figure (2.3) and photographic view in Fig. (2.2(a) to (c)). A componentwise description of the experimental set-up is as follows:

2.3.1 WATER STORAGE TANK

The water body is simulated by a tank of size 570 x 570 x 425 mm deep, fabricated from 12.7 mm thick perspex sheet. For discharge and intake, holes were drilled at various positions as shown in Fig. 2.4(a). Intakes not under use were kept closed. The tank walls and bottom were insulated with 25 mm thick thermocole sheets with a view to minimize heat losses from walls and bottom to surroundings.

2.3.2 WATER CIRCULATION ARRANGEMENT

Warm water was discharged at the top of the water body having cool water intake at the lower level. Teflon tubes, insulated with thermocole, were used for all the connections. The steady flow of hot water in the discharge line was achieved by an adjustable constant head device, Fig. 2.4(b). The flow rate was measured with the help of a calibrated rotameter. It is worthwhile to mention that the direct control of steady hot water flow rate, even with the help of most sensitive valve was found to be unreliable. At

intake, the rotameter was mounted in between intake point and constant temperature bath (kept at level lower than the tank). The desired flow rate, equal to discharge rate was achieved by adjusting a Hoke valve.

To simulate with hot water circuit of thermal power plant, an ultrathermostatic bath (Temperature range: - 30 to 200°C ; capacity : 15 litres, control accuracy : ± 0.03°C ; heating capacity : 1500 W) was used. The desired temperature of the warm water could be achieved by adjusting a mercury-in-contact thermometer having an on-off heater control.

2.3.3 ARRANGEMENTS FOR TEMPERATURE MEASUREMENT:

Temperatures were recorded using 20 gage copper - constanton and 36 gage Alumel - chromel thermocouple wires. Ordinary copper wire was used for extension from thermocouples to calibrated temperature indicator potentiometer.

For the study of stratification in the water body, 36 thermocouples were fixed in four horizontal planes, each plane having 9 thermocouples. In addition, 15 thermocouples were placed uniformly at the water surface, Fig. 2.4(c). Separate thermocouples were used to get intake, discharge and atmospheric temperatures.

A moving probe, exhibited as in Fig. 2.4(d) consists 10 thermocouples glued to two 2 mm thick copper sticks.

It was mounted on a sliding stand having movement along the jet direction in the horizontal plane. The probe itself slides laterally (perpendicular to jet direction) and vertically on this stand. This arrangement facilitated the measurement of temperature at any desired location in the tank. Measuring scales were fitted to locate any point of interest in the tank.

2.3.4 TEMPERATURE INDICATOR POTENTIOMETER

A 48-point Honeywell temperature indicator potentiometer was used for successive temperature measurements. It was pre-set for copper-constanton thermocouples and had a measuring accuracy of 0.15°C. The indicator scale was, however, calibrated for alumel-chromel thermocouples.

A 20-point temperature recorder was used to record continuous variations of surface temperature at the beginning of the experiment. The values were recorded graphically within an accuracy of $\pm$ 1°C.

2.3.5 SURFACE AIR DISCHARGE ARRANGEMENT

It consists of a blower mounted at the upper level of the tank. The air was supplied through a round duct having ractangular exit (600 x 130 mm deep) placed near the tank. To have uniform air stream, wire-mesh strainer was put in the duct. The desired wind velocity (in the range of

4 to 16 Km/h) was maintained by regulating the supply voltage of the blower.

2.4. EXPERIMENTAL PROCEDURE:

2.4.1. RANGE SELECTION

To simulate water bodies having usual depth 15 to 30 m , depth ratio (Z_r) is taken to be 1/30 to 1/60. Subsequently velocity ratio should vary between 0.13 to 0.18. For prototype systems, Reynolds number (Re_p) is of the order of 10^6 and discharge velocity vary between 0.2 to 0.4 m/s. The ranges for model Reynolds number (Re_m) and jet velocity are found to be 2000 to 6000 and 1.1 to 3.0 m/s, respectively. Hence, jet diameter (d_o) is taken to be d_o = 1.3 mm and hot water flow rate 100 to 200 ml/min.

Densimetric Froude number limit the temperature rise at intake (ΔT_i). Therefore, ΔT_i is selected as 10 to 20°C, the normal range of condenser temperature rise in a power plant.

2.4.2 PROCEDURE

First, the storage tank is filled upto desired level with water at ambient temperature. Heater in ultra-thermo-static bath is put on, and murcury-in-contact-thermometer adjusted to give preselected temperature rise at the discharge point.

Height of the constant head device is adjusted to yield desired hot water flow rate, as checked by rotameter. The same flow rate is maintained at intake by proper opening of Hoke Valve.

All the temperatures, inside the tank and at the surface of the water, are measured and recorded at 1/2 to 2 hour interval, depending upon the case. Measurements are continued till a steady-state, which occurred in 6 to 12 hours, is achieved.

Variations in intake temperature and depth of buoyant pool are observed for a number of discharge conditions and intake locations. Finally, experiments are conducted for a set of wind velocities to determine heat and mass-transfer coefficients.

CHAPTER-3

ANALYTICAL STUDY

3.1 DESCRIPTION:

At steady state meteorological conditions, the water surface eventually reaches an equilibrium temperature (T_e) for which the net heat-flux at the interface is zero. But in practice, the water body is subjected to rapid variations in meteorological data. Hence its equilibrium temperature has large fluctuations even for a single day. However, it always try to reach T_e asymtotically with time due to thermal inertia. Therefore, the actual temperature attained by the water body, called as natural water temperature (T_n), has very small fluctuation compared to T_e.

The temperature distribution of the water body alters in presence of a heat source. This gives rise to an excess temperature (ΔT) over T_n, and is determined with the help of energy balance equation.

3.2 ENERGY BALANCE EQUATION

The net short-term heat exchange across a unit area of the surface per unit time, Q (T,t), can be expressed as:

$$Q\ (T,t) = Q_G\ (t) + Q_a\ (t) - Q_b\ (T) - Q_e\ (T,t) - Q_c\ (T,t) \qquad (3.2.1)$$

where

T = surface temperature of water (°K)

$Q_G(t)$ = heat gain by short-wave radiations absorbed by water at time t (W/m^2)

$Q_a(t)$ = heat gain by long-wave atmospheric radiations absorbed by water at time t (W/m^2)

$Q_b(t)$ = heat loss due to back radiations at time t (W/m^2)

$Q_e(T,t)$= heat loss due to evaporation (W/m^2)

$Q_c(T,t)$= heat loss due to convection (W/m^2).

$Q_G(t)$ is directly known from radiation data. Remaining quantities can be obtained in terms of natural water temperature and meteorological variables as follows:

3.2.1 ATMOSPHERIC RADIATION

The estimation of atmospheric radiation is extremely complex due to involvement of moisture, temperature, ozone, carbon dioxide etc. However, using weather observations, it is expressed as [1]:

$$Q_a\ (t) = 0.97 \cdot \sigma \cdot \beta \cdot T_a^4 \qquad (3.2.2)$$

where $\beta = 0.75$ to 0.85

3.2.2. BACK RADIATION

Long wave radiations emitted by a water surface can be computed from the well-known Stefan-Boltzman law for the black body radiation :

$$Q_b\ (t) = 0.97 \cdot \sigma \cdot T^4 \qquad (3.2.3)$$

3.2.3. EVAPORATION

It is caused due to the difference between the vapor pressures at water surface and ambient air. Its magnitude depends upon air temperature, humidity and wind speed etc. The heat-transfer by evaporation is, however, evaluated from

$$Q_e\ (T,t) = h(W) \cdot [E(T) - E_a(t)] \cdot L(T) \qquad (3.2.4)$$

where,

$h(W)$	=	mass-transfer coefficient = (a+bW) 'a' and 'b' are constants
W	=	wind velocity (km/h)
$E(T)$	=	saturated vapor pressure of air at temperature 'T' (bar)
$E_a(t)$	=	vapor pressure of ambient air (bar) = ϕ, $E(T_a)$
ϕ	=	relative humidity
$L(T)$	=	enthalpy of evaporation at temperature 'T'. (KJ/kg)

3.2.4. CONVECTION

On the basis of heat and mass transfer similarity the ratio Q_c / Q_e has been given by Boven [16] as :

$$Q_c / Q_e = 0.61 \times 10^{-3} \cdot (T-T_a) / [E(T) - E_a] \quad (3.2.5)$$

hence,

$$Q_c (T,t) = 0.61 \times 10^{-3} \cdot h(W) \cdot [T-T_a(t)] \cdot L(T) \quad .... \quad (3.2.6)$$

The overall expression for heat-exchange at water surface takes the form:

$$Q (T,t) = Q_G(t) + 0.776 \cdot \sigma \cdot [T_a(t)]^4 - 0.97 \cdot \sigma \cdot T^4 - h(W) \cdot [E(T) - \phi \cdot E(T_a)] \cdot L(T) - 0.61 \times 10^{-3} \cdot h(W) \cdot (T-T_a) \cdot L(T) \quad (3.2.7)$$

with,

$$E(T) = .0233.8 \text{ EXP } [18.1 - 5303.3/T] \quad (3.2.8)$$

$$L(T) = (3145.99 - 2.368 \cdot T) \cdot 10^3 \quad (3.2.9)$$

3.3 EXCESS TEMPERATURE (ΔT):

Heat balance equation is separated into two components that is, first term represents heat-flux caused naturally while the other accounts for heat loading. Using $T = T_n + \Delta T$, one can express:

$$Q (T,t) = Q (T_n + \Delta T, t)$$

$$= Q (T_n, t) + \int_{T_n}^{T_n+\Delta T} Q_T (T,t).dt \quad (3.3.1)$$

where,

$Q\ (T_n,t)$ = heat-transfer at natural water temperature, T_n

$$Q_T(T,t) = \partial Q\ (T,t) / \partial T \qquad (3.3.2)$$

Second term on R.H.S. of Eq. (3.3.1) may be integrated numerically using Trapezoidal rule as :

$$\int_{T_n}^{T_n+\Delta T} Q_T\ (T,t)\ .\ dt = \frac{\Delta T}{2}\ .\ [Q_T\ (T_n\ ,\ t) + Q_T\ (T_n+\Delta T,t) \qquad \ldots\ (3.3.3)$$

For a preliminary estimate of ΔT, Eq. (3.2.7) is linearized taking T_n as the base temperature.

$$Q\ (T_n + \Delta T,\ t) = Q\ (T_n,t) + \Delta T\ .\ Q_T\ (T_n\ ,\ t) \qquad \ldots\ (3.3.4)$$

Using Eq. (3.2.7), Eq. (3.3.4) is expressed as

$$\begin{aligned} Q\ (T_n + \Delta T,t) = Q\ (T_n\ ,\ t) &- 3.88\ .\ \sigma\ .\ T_n^3 \\ &- h(W).[L(T_n).E_T\ (T_n) + \\ &L_T\ (T_n).[E\ (T_n) - \phi\ .\ E\ (T_a)]].\Delta T \\ &- 0.61 \times 10^{-3}\ .\ h(W).[L\ (T_n) \\ &+ L_T\ (T_n).[\ T - T_a\ (t)]].\Delta T \end{aligned} \qquad (3.3.5)$$

where,

$$E_T\ (T_n) = \partial E(T)/\partial T \Big|_{T=T_n} = 5303.3\ .\ E(T)/T^2 \qquad \ldots\ (3.3.6)$$

$$L_T\ (T_n) = \partial L(T)/\partial T \Big|_{T=T_n} = -\ 2368 \qquad (3.3.7)$$

Using an overall surface heat transfer coefficient (K; W/m^2-K), Eq. (3.3.5) is expressed as

$$Q\ (T_n + \Delta T, t) = Q\ (T_n, t) - K\ .\ \Delta T \qquad (3.3.8)$$

with,

$$K = K\ (T_n, t) = -\ Q_T\ (T_n, t) = K_b + K_e + k_c \qquad (3.3.9)$$

K_b = back radiation heat-transfer coefficient

$$= 3.88\ .\sigma\ .\ T_n^3 \qquad (3.3.10)$$

K_e = evaporation heat-transfer coefficient

$$= h(W)\ [L(T_n).E_T(T_n)+L_T(T_n).[E(T_n)-\emptyset.E(T_a)]] \qquad (3.3.11)$$

...

K_c = convection heat-transfer coefficient

$$= 0.61 \times 10^{-3}\ .\ h(W).[L(T_n)+ L_T(T_n).[T-T_a(t)]] \qquad (3.3.12)$$

...

Equation (3.3.8) gives the value of excess temperature as:

$$\Delta T = QP/K \qquad (3.3.13)$$

where,

QP = plant heat load $(W/m^2) = Q(T_n, t) - Q(T_n + \Delta T, t)$

Excess temperature predicted by Eq. (3.3.13) is used together with Eq. (3.3.3) to iterate for actual temperature rise ($\Delta T'$)

$$\Delta T' = 2\ .\ QP/[K(T_n, t) + K(T_n + \Delta T, t) \qquad (3.3.14)$$

At known natural water temperature and meteorological conditions, Eqs. (3.3.13 and 14) are used to determine temperature rise at the surface for the given plant heat load.

3.4 DIFFERENTIAL EQUATIONS AND METHOD OF SOLUTION:

In developing the differential equations following assumptions are made:-

1. Energy transfer across sides and bottom of the water body is insignificant.
2. Temperature variations occur only in the vertical direction. Horizontal gradients are negligible. They are adequately supported by the experimental results.
3. Water body is ractangular.
4. Properties such as ρ , c_p, etc. are constant.

3.4.1 DIFFERENTIAL EQUATIONS:

The thermal-energy stored by water, relative to that contained at a base temperature (T_B), is given:

$$\text{Energy} = c_p \, , \, \rho \, [(T_n + \Delta T) - T_B]$$

The conservation of thermal-energy equation for a differential volume of water is ;

$$\frac{\partial [(T_n + \Delta T) - T_B]}{\partial t} = \varepsilon_z \frac{\partial^2 [(T_n + \Delta T) - T_B]}{\partial z^2} \qquad \ldots \quad (3.4.1)$$

that is,

$$\frac{\partial(T_n - T_B)}{\partial t} + \frac{\partial(\Delta T)}{\partial t} = \varepsilon_Z \frac{\partial^2(T_n - T_B)}{\partial Z^2} + \varepsilon_Z \frac{\partial^2(\Delta T)}{\partial Z^2} \quad \ldots \quad (3.4.2)$$

Boundary conditions:

$$\text{At} \quad Z = 0 \; : \; \varepsilon_Z \frac{\partial(T_n + \Delta T - T_B)}{\partial Z} = - \frac{Q(T,t)}{\rho \cdot c_p} \quad \ldots\ldots \quad (3.4.3)$$

$$\text{At} \quad Z = H \; : \; \varepsilon_Z \frac{\partial(T_n + \Delta T - T_B)}{\partial Z} = 0 \quad (3.4.4)$$

An equation similar to Eq. (3.4.1) is derived for the distribution of natural water temperatures:

$$\frac{\partial(T_n - T_B)}{\partial t} = \varepsilon_Z \frac{\partial^2(T_n - T_B)}{\partial Z^2} \quad (3.4.5)$$

Boundary conditions:

$$\text{At} \quad Z = 0 \; : \; \varepsilon_Z \frac{\partial(T_n - T_B)}{\partial Z} = - \frac{Q\,(T_n\,,\,t)}{\rho \cdot c_p} \quad (3.4.6)$$

With $Q\,(T_n,t)$ from Eq. (3.2.7) and

$$\text{At} \quad Z = H \; : \; \varepsilon_Z \frac{(T_n - T_B)}{Z} = 0 \quad (3.4.7)$$

Since the natural water temperature distribution is independent of the excess temperature, the distribution of ΔT can be had by substracting Eq. (3.4.5) from Eq. (3.4.2). It gives :

$$\frac{\partial(\Delta T)}{\partial t} = \varepsilon_Z \frac{\partial^2(\Delta T)}{\partial Z^2} \quad (3.4.8)$$

With Boundary Conditions:

$$\text{At} \quad Z = 0 \; : \; \varepsilon_{Z_{\Delta T}} \left[\partial (\Delta T) / \partial Z \right] = K \cdot \Delta T / \rho \, c_p \quad \ldots \quad (3.4.9)$$

$$\text{and} \quad Z = H \; : \; \varepsilon_{Z} \left[\partial (\Delta T) / \partial Z \right] = 0 \quad (3.4.10)$$

3.4.2 METHOD OF SOLUTION:

Equations (3.4.5 and 3.4.8) are solved numerically to get natural and excess temperature distribution. Heat-transfer across the surface is calculated using hourly meteorological data. The cooling water body is divided into 'n' horizontal elements, each of depth ΔH. Finite difference equations are written for each element. (Appendix-I). Since time step is one hour, the necessary requirement of convergence is fulfilled by a proper selection of depth step. Eq. 3.4.5 is solved by iterative technique for hourly natural water temperature distribution in the water body. Iteration is continued until the convergence is obtained, indicated by a small difference (0.01 to 0.1°C) between $T_n^{p+1}(I)$ and T_n through out the year, for all values of I considered. (p is the number of iteration and I is the number of the depth element from the top). Initial guess of T_n^0 (I) is found to affect convergence significantly. If the water body is taken to be at constant temperature and boundary conditions are imposed suddenly, there will be high values of flux near the surface.

Therefore, the values of $\partial T_n / \partial z$ computed during the first few steps in time will be very inaccurate. Hence instead of constant values at t = 0, the iteration is started from a computed solution at t = 10 to 12-hours.

Excess temperatures at the surface throughout the year are calculated using T_n at the surface and Eqs. (3.3.13 and 14). Eq. (3.4.8) is then solved by iterative technique. A linear excess temperature distribution as an initial guess is found to give rapid convergence.

CHAPTER-4

RESULTS AND DISCUSSION

Experimental investigation has been carried out to study the temperature characteristics at intake with respect to its location, pond depth, plant and meteorological variables for transient and steady conditions. Following dimensionless quantities are used to represent variables:

Dimensionless intake temperature: $\bar{T}_o = (T_o - T_a)/(T_i - T_a)$ ... (4.1)

Dimensionless time : $\tau = \alpha\, t / H^2$ (4.2)

where,

T_o = intake temperature (°K)

T_a = atmospheric temperature (°K)

T_i = inlet temperature (°K)

t = time (s)

H = pond depth (m)

α = thermal diffusivity (m^2/s)

4.1 INTAKE TEMPERATURE ($\bar{T}_o$)

4.1.1. EFFECT OF INTAKE POSITION

Figures 4.1 and 2 indicate the transient behavior of temperature at intake for its various positions. It ($\bar{T}_o$)

rises exponentially with time, having lower value at deeper intake and vice-versa. The difference in $\bar{T}_o$ values of two consecutive intakes in a vertical plane is observed to decrease with decreasing depth. Therefore, a deeper intake should be preferred.

At higher flow rate (or Re), the temperature rise is more at all levels. The effect becomes pronounced towards th free surface. It is because the mixing in the upper region is much more at higher Re. The experimental results suggest that the mixing is, further, accelerated by placing intake in this region.

4.1.2 EFFECT OF HOT WATER FLOW RATE ($\dot{m}$)

The variation of intake temperature, at different flow rates and discharge temperature rise ΔT_i = 10 and 15°C for a typical intake position, is exhibited in Figs. 4.3 and 4. It is observed that intake temperature augments with increasing $\dot{m}$. The change in steady temperature with an increase in flow rate from $\dot{m}$ to 1.5 $\dot{m}$ is double than that for increase in $\dot{m}$ from 1.5 $\dot{m}$ to 2.0 $\dot{m}$. It is because of more mixing at higher flow rate.

4.1.3 EFFECT OF DISCHARGE TEMPERATURE RISE (ΔT_i)

Transient variations of intake temperature for a flow having Reynold number of 4900, and ΔT_i = 10, 15 and 20°C

are shown in Fig. 4.5. The increase in ΔT_i does not produce a proportionate increase in $\bar{T}_o$. It is because the heat dissipation across the water surface increases due to higher ΔT_i, 10 to 15°C, resulting in a corresponding low temperature rise at intake. On further increase in ΔT_i, that is, from 15°C to 20°C, the available surface of the water body is not adequate to dissipate the heat proportionately. It results in elevated intake temperature due to heat accumulation. Therefore, ΔT_i more than 15°C for such a water body (corresponding to a heat loading of 600 W/m^2 or more) should not be employed. However, for the same heat discharge, a temperature rise between 10-15°C and correspondingly higher flow rate is a better choice.

Figure 4.6 exhibits an overall summary of steady state intake temperatures under various discharge conditions. It is evident that a higher temperature rise (between 10 - 15°C) and Reynolds number (Re_m = 3000 to 5000) are a suitable choice if regulatory measures of temperature rise are within satisfactory limits. For Re_m less than 3000, ΔT_i should be kept below 10°C.

4.1.4 EFFECT OF POND DEPTH

In practice, several types of water bodies having different shapes and depths are encountered. However, depth is an important parameter. Fig. 4.7 shows the effect

of pond depth on intake temperature. It is seen that in shallow ponds temperature increases quickly and eventually becomes almost uniform. It implies, therefore, that intake can be located anywhere except in the vicinity of the discharge point. The above results have been found to be true for all the operating ranges.

4.2 POOL FRACTION (IP)

Experimental results reveal that a buoyant pool is established in the upper part of the water body. The temperatures below it vary mildly and seldom exceed 10% of intake temperature rise. For practical purposes, a water body can be divided into two distinct layers, the upper one being warmer and lower one cool. The variation of pool fraction (IP : expressed as the ratio of warm layer to the total pond depth) for various discharge conditions and intake locations are displayed by Fig. 4.8[17]. Depth of warm layer increases with increasing flow rate (or Re) due to enhanced momentum causing mixing. The position of intake point has important influence on the value of IP. At bottom intake, IP decreases with increasing ΔT_i while at top intake, the behavior is reverse. Temperature for bottom intake is comparatively low due to longer flow path. Also the higher value of ΔT_i causes larger heat dissipation from the water surface. It results in proportionately low temperature build-up of the water body, rendering a reduction

in IP. At top intake, $\bar{T}_o$ which corresponds to the surface temperature, is quite high. A major portion of heat supplied is carried by the intake water. It decreases the heat loss from the surface. The water body is thus subjected to heat accumulation which, in turn, results in deeper warm water layer. This tendency becomes pronounced as the temperature rise at discharge increases.

4.3 EFFECT OF WIND VELOCITY (W)

The steady state structure established in a water body gets disturbed due to meteorological variables like wind velocity, air temperature and relative humidity etc. A typical nature of intake temperature variation with wind velocity is exhibited in Fig. 4.9 for $Re_m = 5000$. It shows exponential decreament in $\bar{T}_o$ with increasing W. The graph signifies the importance of considering meteorological parameters for the analysis of water bodies.

Since experimentation is not possible in transient environments, an analytical solution is required. At zero wind velocity, the natural convection and diffusion govern the surface temperature. Heat-transfer across the interface increases at higher wind velocities. Surface temperatures are obtained experimentally for various cases. Heat and mass transfer coefficients are then calculated from energy balance equation. Fig. 4.10 shows the variation of mass

transfer coefficient with wind velocity. A linear profile is selected. Values reported by Yotsukura et al [4] are low as effect of natural evaporation has been neglected. h(W) obtained by experimental results match well with its values reported by Ryan et al [3].

4.4 ANALYTICAL RESULTS

Using hourly values of meteorological data of N.Delhi [18], transient variations of daily average natural water temperature are presented in Fig. 4.11. The changes in temperature with depth are not large because of mixing caused by wind currents etc.

In Fig. 4.12, transient variations in excess temperature at the surface (ΔT) are shown. ΔT is minimum in June, July and maximum in December, January. It is because during winter, T_n is low. At low temperature, heat dissipation from the surface is less. Therefore, to dissipate the plant heat, the surface temperature should elevate. Reverse is the case for summer. As the heat load increases, ΔT also increases, but not proportionately, as seen from Fig. 4.12. Error of linearization is more for higher ΔT but for a temperature rise of few degrees (2 to 4°C) it is almost negligible.

Figure 4.13 exhibits the transient distribution of excess temperature in a water body, for a plant load of 100 W/m^2. Sharp gradients occur near the surface and comparatively less fluctuations are observed at lower depths. The net temperature distribution can be had by summing up T_n and ΔT due to a certain plant load, at each location.

Excess temperatures are predicted using an overall surface heat-transfer coefficient (K) defined by Eq. (3.3.13). Fig. 4.14 shows the effect of meteorological variables and T_n on K. It's values for two limiting cases of air-temperature and relative humidity (T_a = 50°C, ϕ = 100% and T_a = 0°C, ϕ = 0 %) are presented. It is evident that T_a and ϕ have almost no influence on the value of overall surface heat-transfer coefficient. Therefore, K may be expressed in terms of wind velocity and T_n only. Generally T_n vary from 10 to 40°C and W from 6 to 20 km/h. Hence, a practical zone of K values (varying between 15 to 90 W/m^2-K) is identified.

K consists of back radiation, evaporation and convection heat-transfer coefficients. It is exhibited from Fig. 4.15 that evaporation is the dominating cause of heat-dissipation. Moreover, it changes largely with wind velocity and T_n.

4.5 ILLUSTRATION:

In the following illustration, present results are used to select the cooling water system of a thermal power plant . Its effect on temperature rise in the water body is also obtained.

Available Information:

1. Ultimate generation capacity of the thermal power plant complex : 5130 MW; using 210 and 500 MW steam turbines.
2. Condenser water cooling : Through the reservoir of a hydel power plant located nearby.

Reservoir Data:

1. Surface Area :
   (a) At maximum water level : 70,000 acre or $2.83 \times 10^8 m^2$
   (b) At minimum water level : 32,000 acre or $1.29 \times 10^8 m^2$
2. Water Storage :
   (a) Live storage at max. water level : 7.28×10^6 acr-ft- or $8.98 \times 10^9 m^3$
   (b) Dead storage: 1.32×10^6 Acr-ft or $1.63 \times 10^9 m^3$

SOLUTION:

Rate of heat conveyed by cooling water: 2×5130

$= 10,260$ MW

Therefore, $\dot{m} = 2.45 \times 10^3$ kg/sec.for $\Delta T_i = 10°C$

$= 1.64 \times 10^3$ kg/sec.for $\Delta T_i = 15°C$

Plant heat load ; QP = 35 to 80 W/m^2

This gives,

$Z_r = 58.8, \quad V_r = 7.67$

and

$$Re_m = 2.216 \times 10^{-3} \cdot Re_p$$

Since Re_m = 3000 to 5000 with a temperature rise of 10-15°C is preferred, the desirable Re_p is obtained as:

$$Re_p = 1.35 \text{ to } 2.25 \times 10^6$$

let diameter of each discharge pipe = 5 m.

Therefore, discharge velocity = 0.24 to 0.4 m/s

discharge flow rate= 4.77 to 8.0 x 10^3 kg/s

Since heat supplied per unit area of the water body is low, the temperature rise of 15°C with a lower water flow rate shall be a suitable choice. Discharge channels can be placed correspondingly.

Now,

Natural water temperature (from Fig. 4.11) : 17.5 to 31°C

Wind velocity : 6 to 13 km/h

Therefore, overall surface heat-transfer coefficient : 18 to 60 W/m^2-k

Approximate excess temperature: 0.58 to 4.4°C

Actual excess temperature (using Fig. 4.12) : 0.5 to 4.0°C

Temperature rise shall be maximum during winter. Since, excess temperature is well within acceptable limits, ecological problems shall not arise.

CHAPTER-5

CONCLUSIONS

From the present study carried out experimentally and analytically the following conclusions are arrived at:

1. A deeper intake allows accelerated mixing at top layer, avoids short circuiting and gives better intake temperature.

2. The higher temperature rise 10 to 15°C and Re_m (3000 to 5000) permits effective utilization of available surface area of the water body, having thermal loading of 200 to 600 W/m^2.

3. In shallow water body, almost uniform water temperature is attained. Therefore, the position of intake is not very critical except in the vicinity of the discharge point.

4. A steady state buoyant pool is established depending upon the discharge conditions. The temperatures in the upper zone are almost constant, while the thermal structure below it remains nearly unaffected.

5. The wind velocity causes sharp decrease in the intake temperature. Therefore, it is important to consider its effect on T_o.

6. Heat and mass-transfer coefficient depends linearly upon wind velocity.

7. The natural water temperature in a water body can be calculated from the meteorological data.

8. The excess temperature can be predicted by linearizing the energy balance equation with natural water temperature as base temperature. Error of linearization is negligible for temperature rise of 4-5°C.

9. Overall surface heat-transfer coefficient, which depends mainly upon the natural water temperature and wind velocity, gives a quick guess of excess temperature at the water surface.

REFERENCES

1. Raphael, J.M. 'Prediction of Temperature in Rivers and Reservoirs', Journal of Power Division, July 1962, pp. 157-180.

2. Edinger, J.E., Duttweiler, D.W., and Geyer, J.C., ' The Response of Water Temperatures to Meteorological Conditions', Water Resources Research, 4 (5), 1968, pp. 1137-1143.

3. Ryan, P.J., Harleman, D.R.F., Stolzenbach, K.D., 'Surface Heat Loss from Cooling Ponds', Water Resources Research, October 1974, pp. 930-938.

4. Yotsukura, N., Jackman, A.P., and Faust, C.R. 'Approximation of Heat Exchange at the Air-water Interface', Water Resources Research, Feb. 1971, pp. 118-128.

5. Jobson, H.E., 'The Dissipation of Excess Heat from Water Systems', J. of Power Division, May 1973, pp. 89-104.

6. Kothandaraman, V.' Analysis of Water Temperature variations in large rivers', J. of Sanitary Division, Feb. 1971, pp. 19-31.

7. Jen, Yuan.,Wiegel, R.L., Mobarek,I.,' Surface Discharge of Horizontal Warm-Water Jet', J. of Power Division, April 1966, pp. 1-28.

8. Tamai, N., Wiegel, R.L., Tornberg, G.F.,' Horizontal Surface Discharge of Warm Water Jets', J. of Power Division, October, 1969, pp. 253-276.

9. Moore, F.K., Jaluria, Y.,' Thermal Effects of Power Plants on Lakes', J. of Heat Transfer, May 1972, pp. 163-168.

10. McGuirk, J.T., Rodi, W.,'Calculation of Three-Dimentional Heated Surface Jets', Heat Transfer and Turbulent Buoyant Convection, Vol. 1, pp. 275-87, 1977.

11. Vasiliev, O.F. 'Three-Dimensional Numerical Model for Hydrothermal Analysis of Cooling Ponds', Thermal Effluent Disposal from Power Generation, pp. 115-132, 1978.

12. Lee, S., Sengupta, S., Tsai, C., Miller, H.' Three-Dimensional Free Surface Model for Thermal Discharge' Waste Heat Management and Utilization, Vol. 3, pp. 1618-1634, 1979.

13. Nystrom, J.B., Hecker, G.E., and Moy, H.C.,' Heated Discharge in an Estuary: Case Study' J. of Hydraulics Division, Nov. 1981, pp. 1371-1406.

14. Jirka, G.H., Watanabe, M. ' Thermal Structure of Cooling Ponds', J. of the Hydraulics Division, May 1980, pp. 701-715.

15. Jirka, G.H., Cerco, C.F., Harleman, D.R.F.' Efficient Cooling Ponds : Design', J. of the Hydraulics Division, Nov. 1981, pp. 1547-1563.

16. Bowen, I.S., 'The Ratio of Heat Losses by Conduction and by Evaporation from any Water Surface', Physical Review, Vol. 27, No. 6, June 1926, p. 785.

17. Agrawal, A.K., Prasad, M.' Heat Rejection from Cooling Water of a Thermal Power Plant by Recirculation in Water Body', Proceedings of the Third Waste Heat Management and Utilization Conference, May 11-13, 1981, University of Miami, U.S.A.

18. Mani, A.' Hand Book of Solar Radiation Data for India', Allied Publishers Pvt. Ltd., 1981.

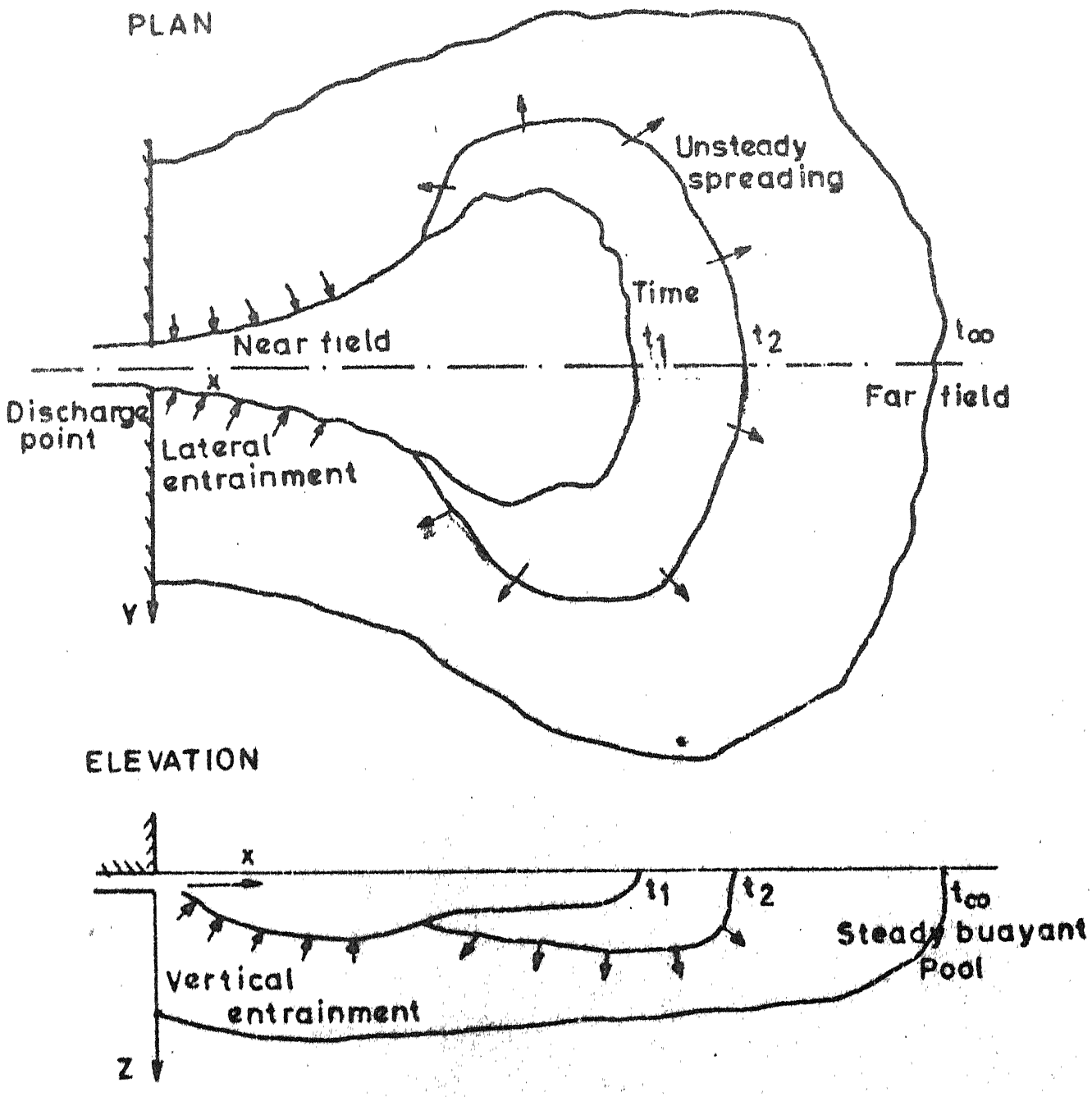

FIG·2·1 STRUCTURE OF BUOYANT JET DISCHARGI
INTO A WATER BODY.

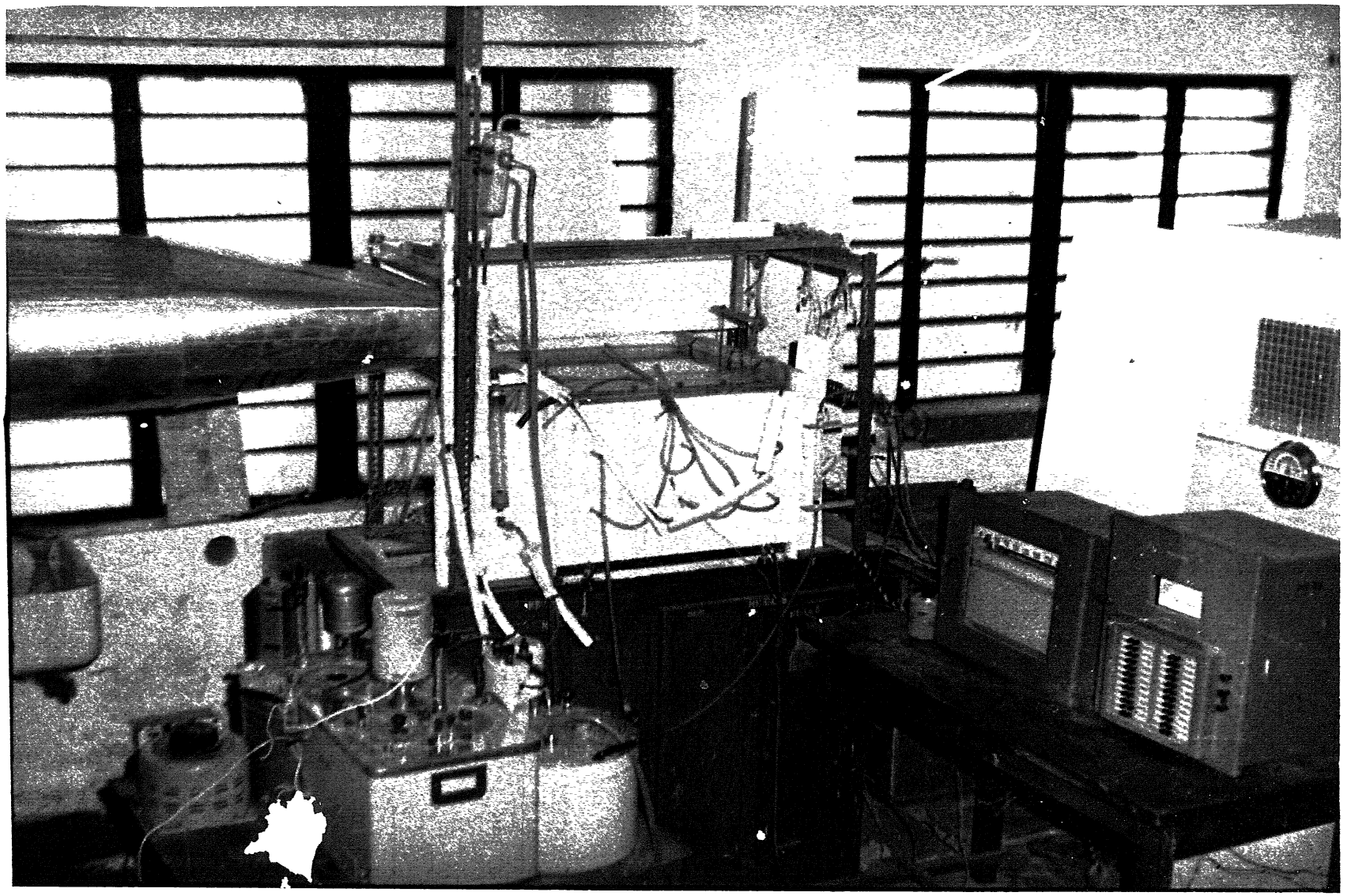

FIG. 2.2 (a) EXPERIMENTAL SETUP

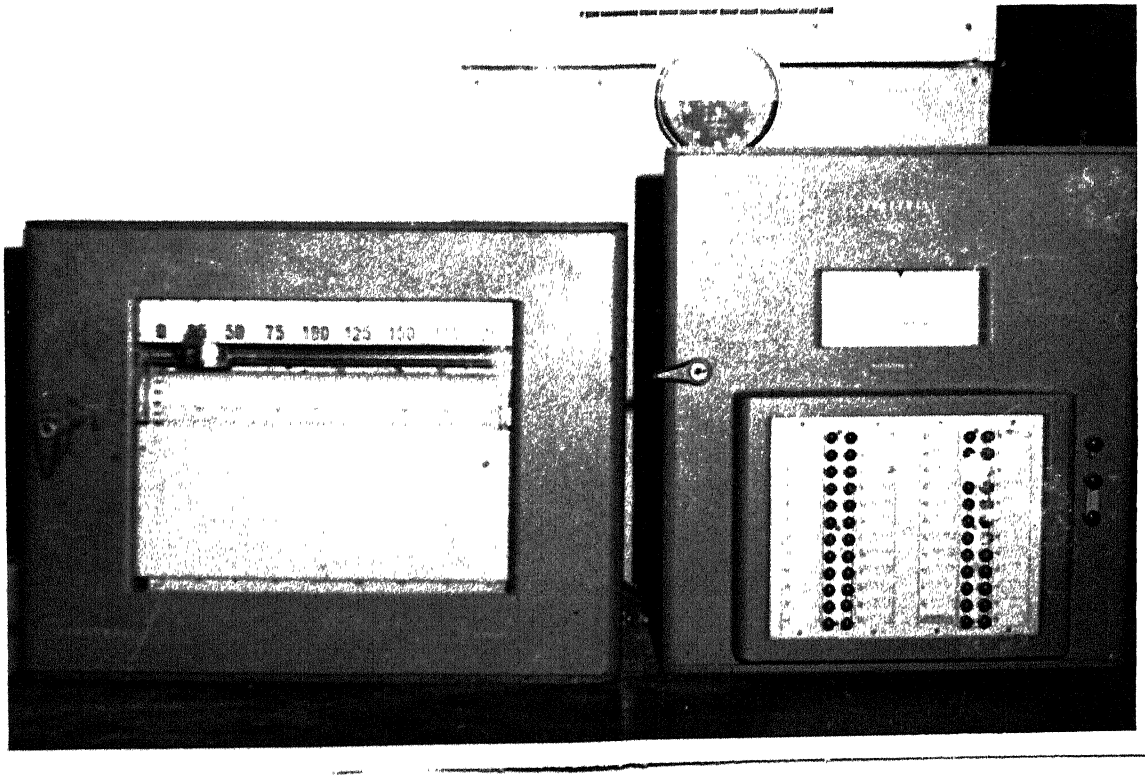

FIG. 2.2 (b) TEMPERATURE MEASURING INSTRUMENTS

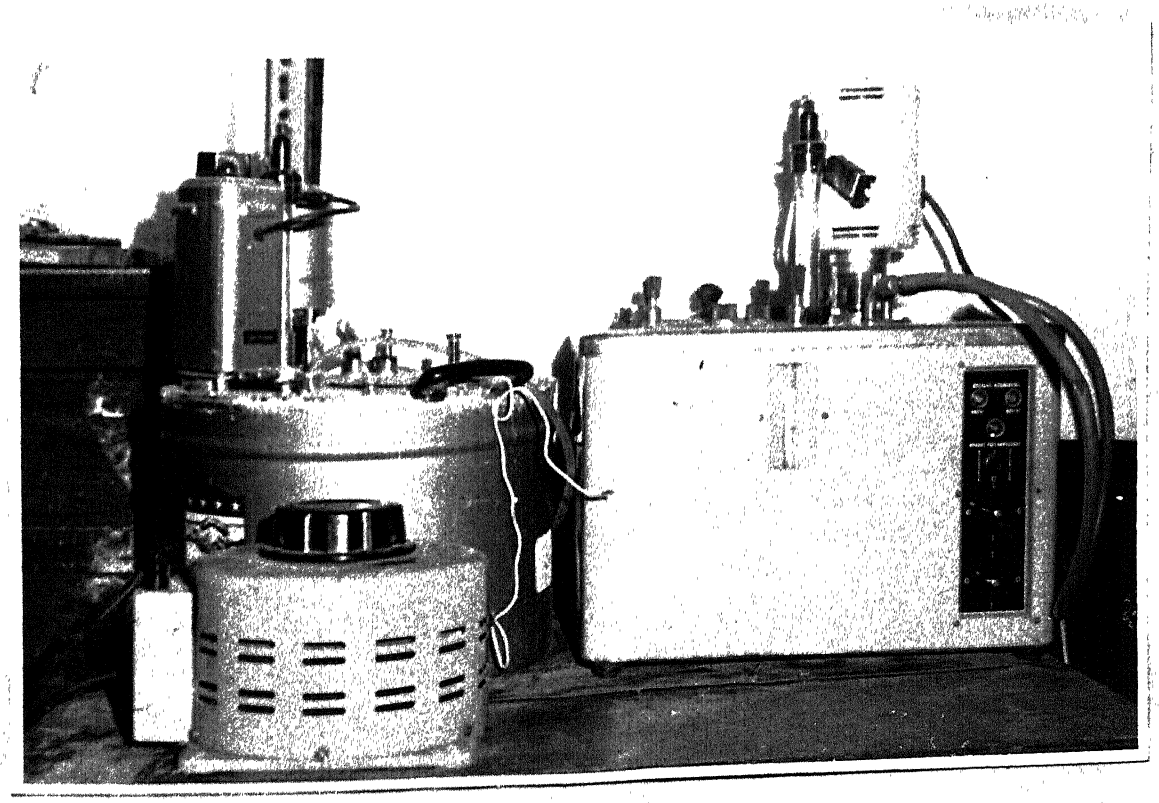

FIG. 2.2 (c) ULTRA-THERMO-STATIC BATH

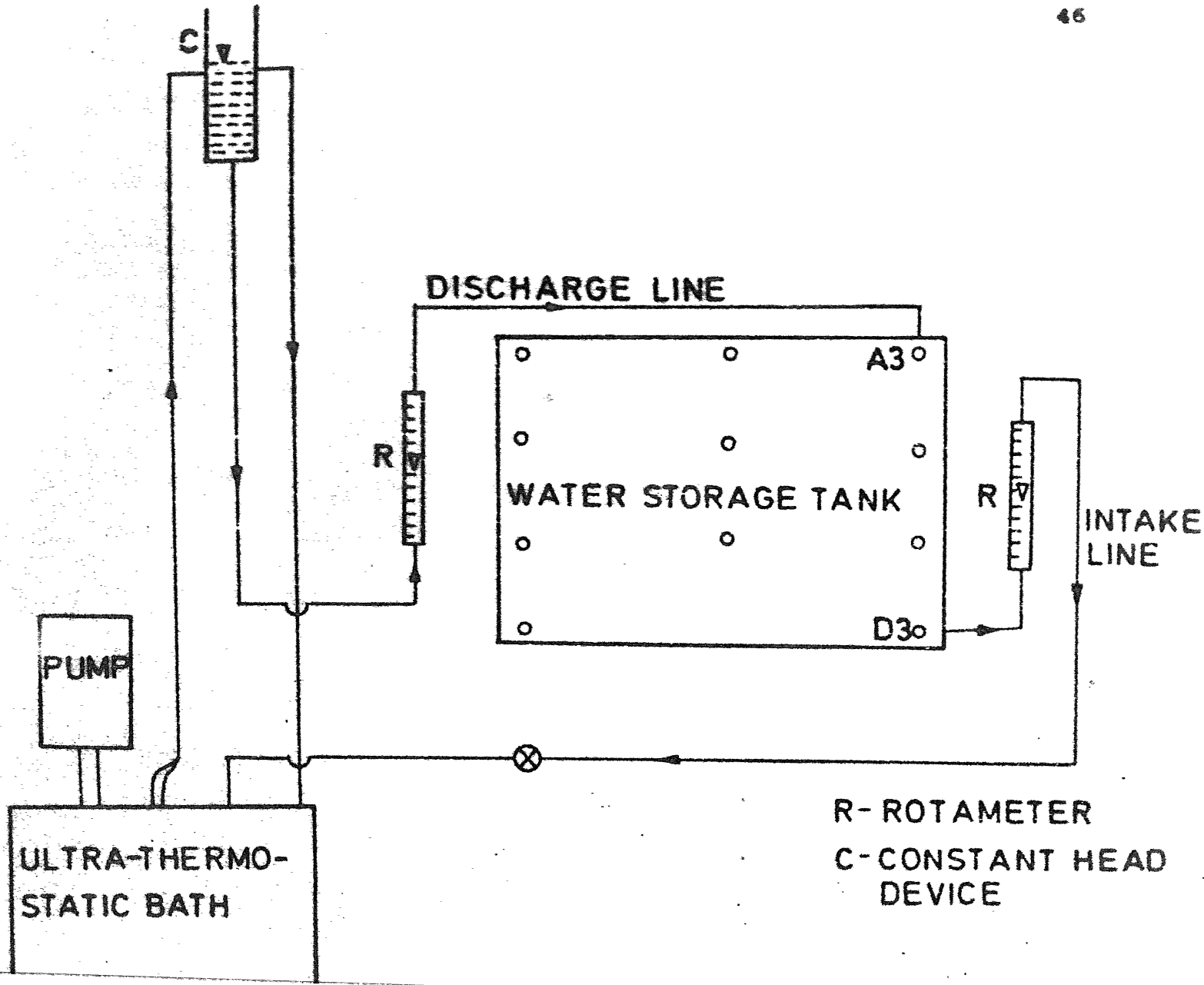
C
DISCHARGE LINE
R
A3
WATER STORAGE TANK
D3
R
INTAKE LINE
PUMP
ULTRA-THERMO-STATIC BATH
R- ROTAMETER
C- CONSTANT HEAD DEVICE

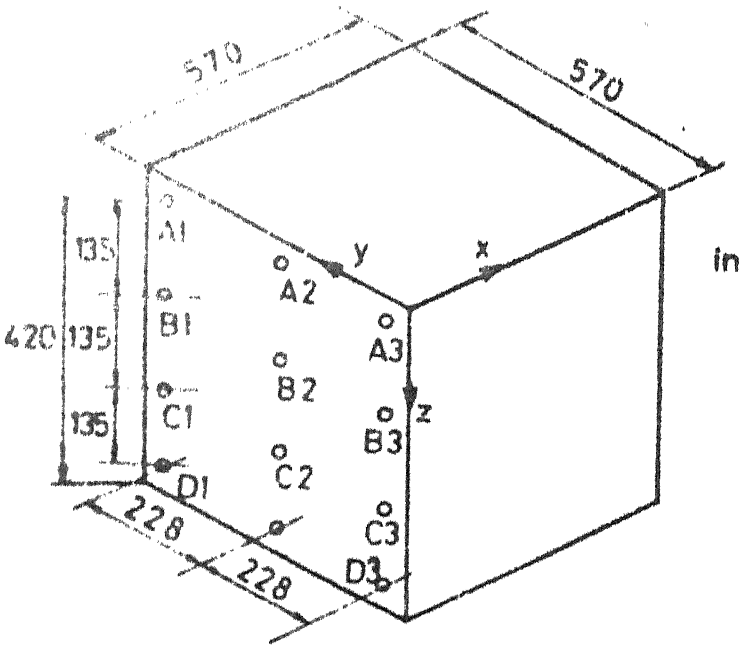

(a) WATER STORAGE TANK

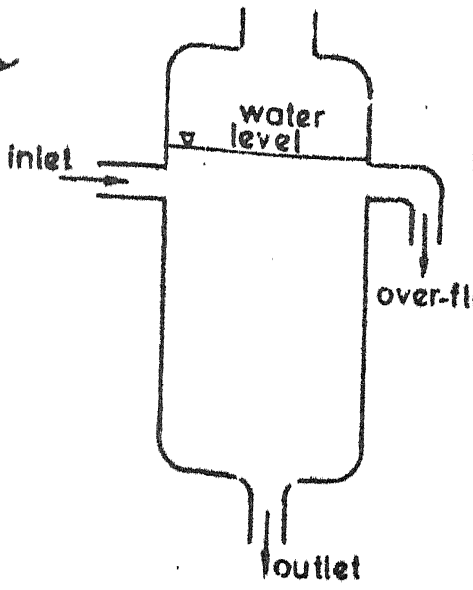

(b) CONSTANT HEAD DEVICE

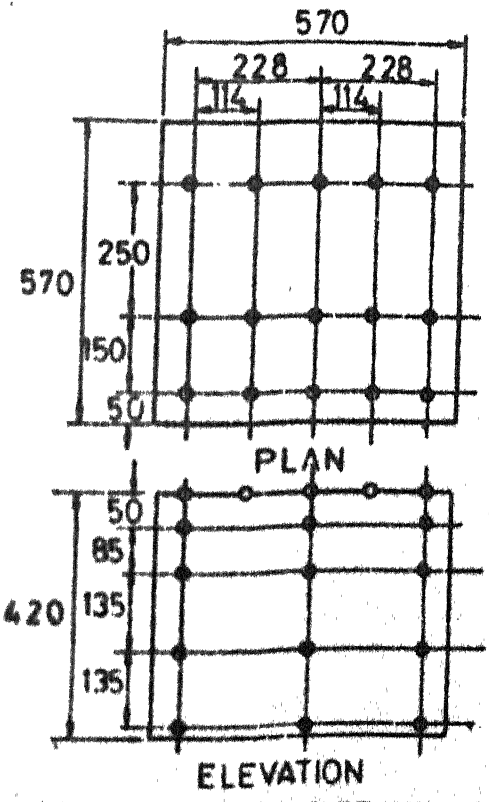

(c) THERMOCOUPLE NET WORK

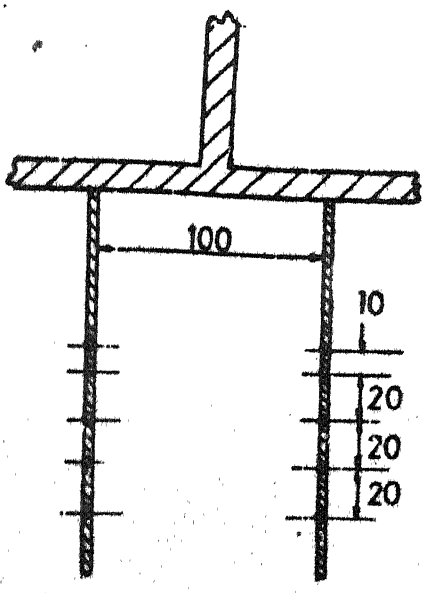

(d) THERMOCOUPLE PROBE

all dimensions are in mm

FIG. 2-4

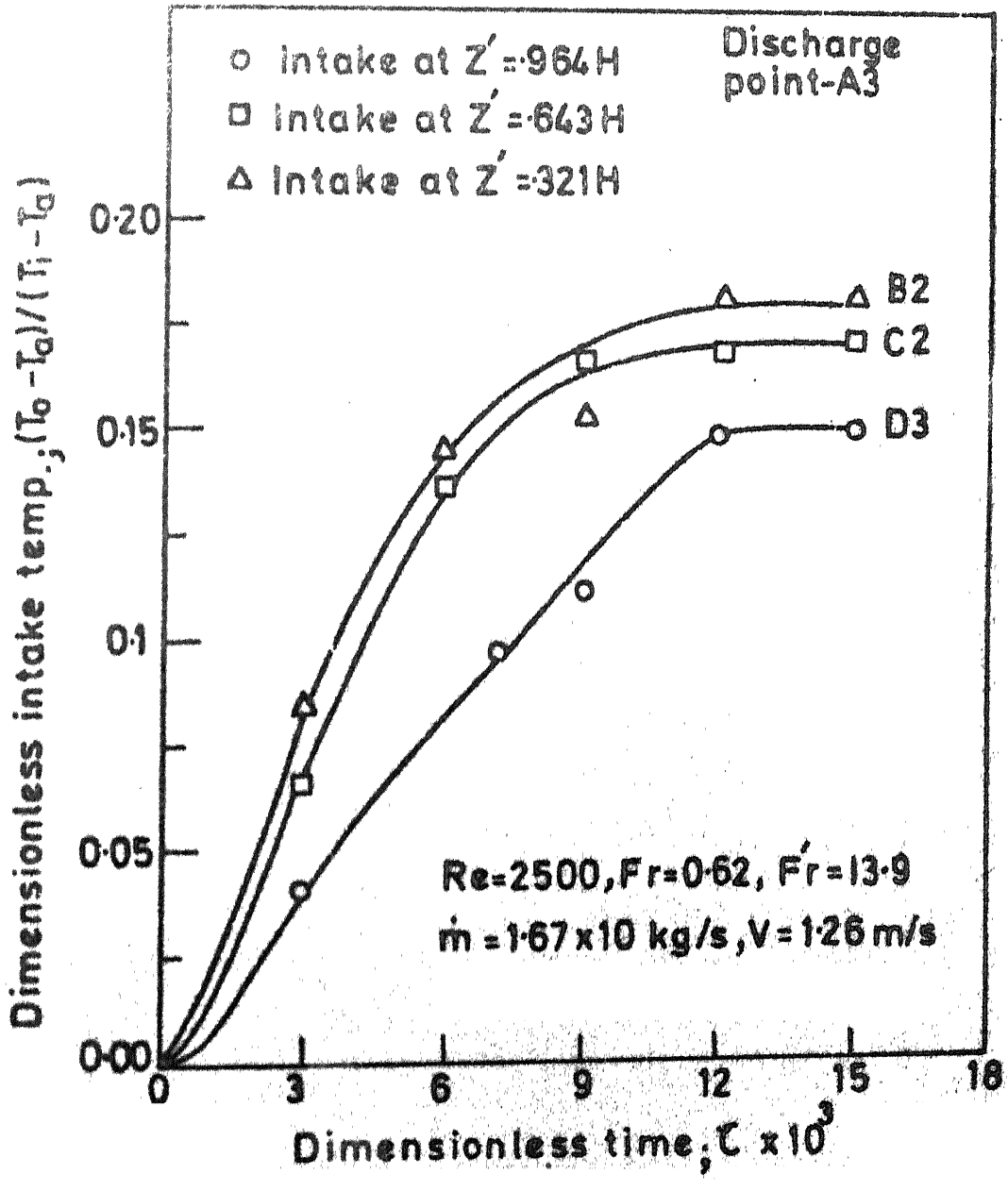

FIG. 4·1 EFFECT OF INTAKE LOCATION ON INTAKE TEMPERATURE.

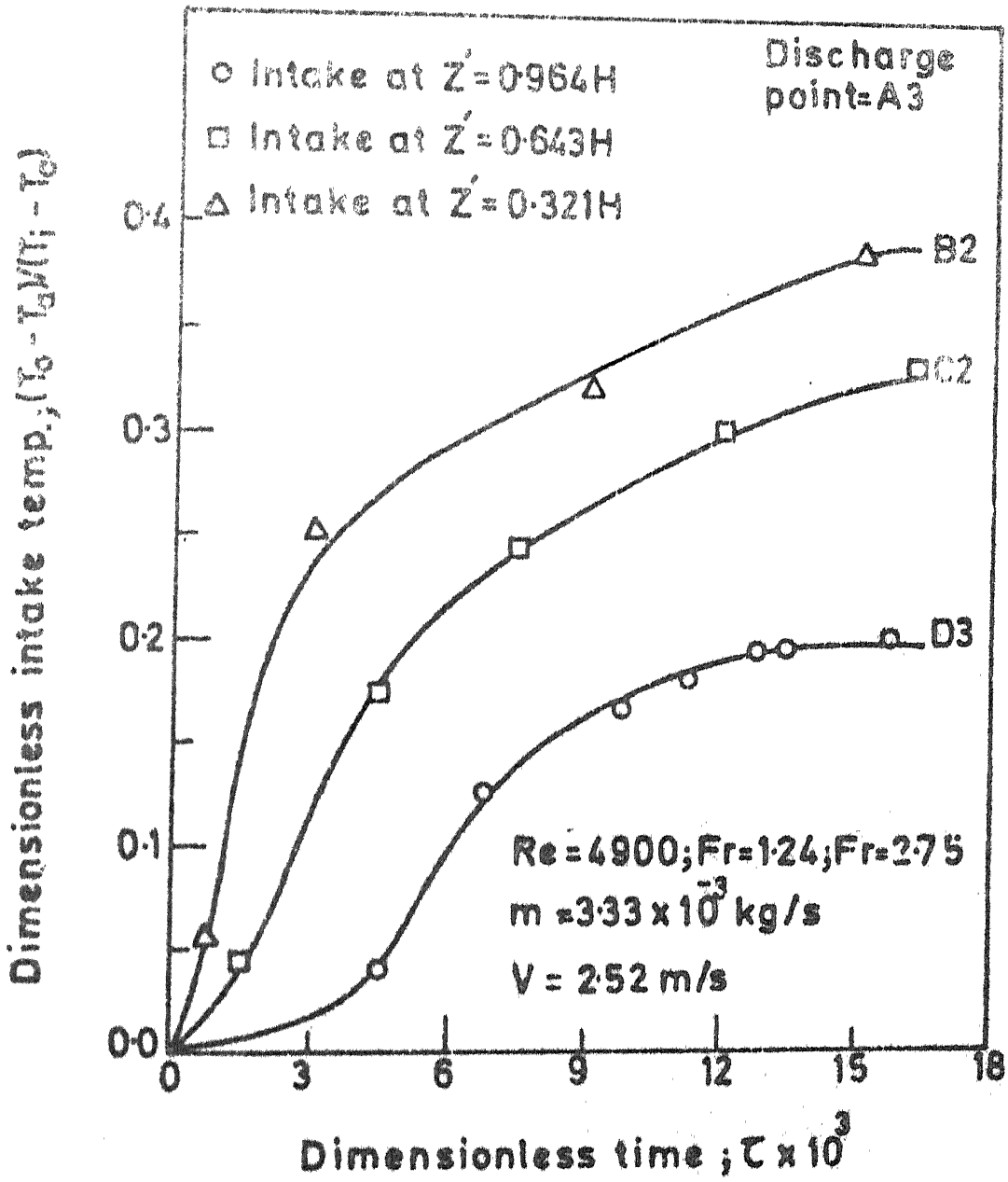

FIG·4·2 EFFECT OF INTAKE LOCATION ON INTAKE TEMPERATURE.

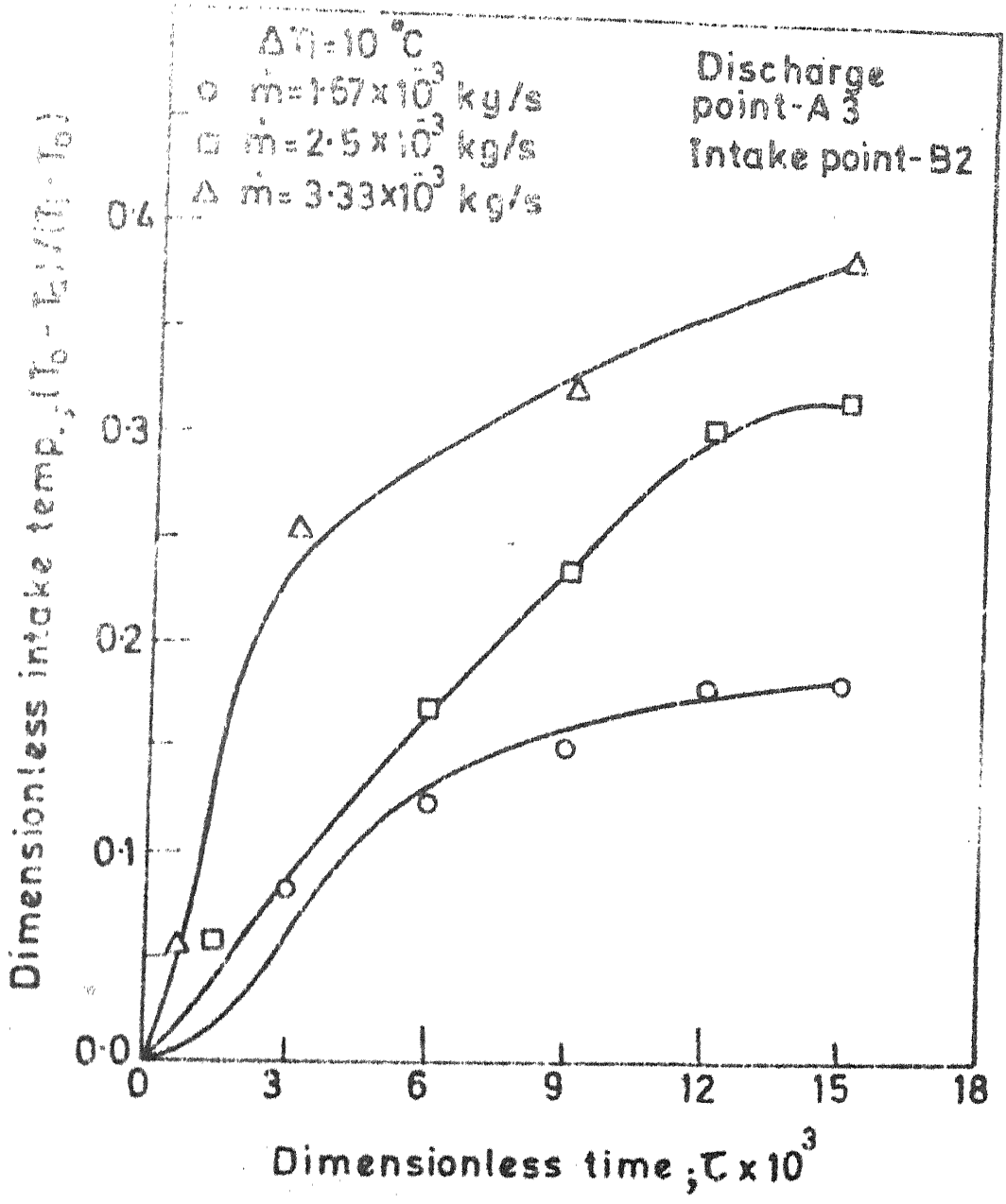

FIG·4·3 EFFECT OF INLET WATER FLOW RATE ON INTAKE TEMPERATURE.

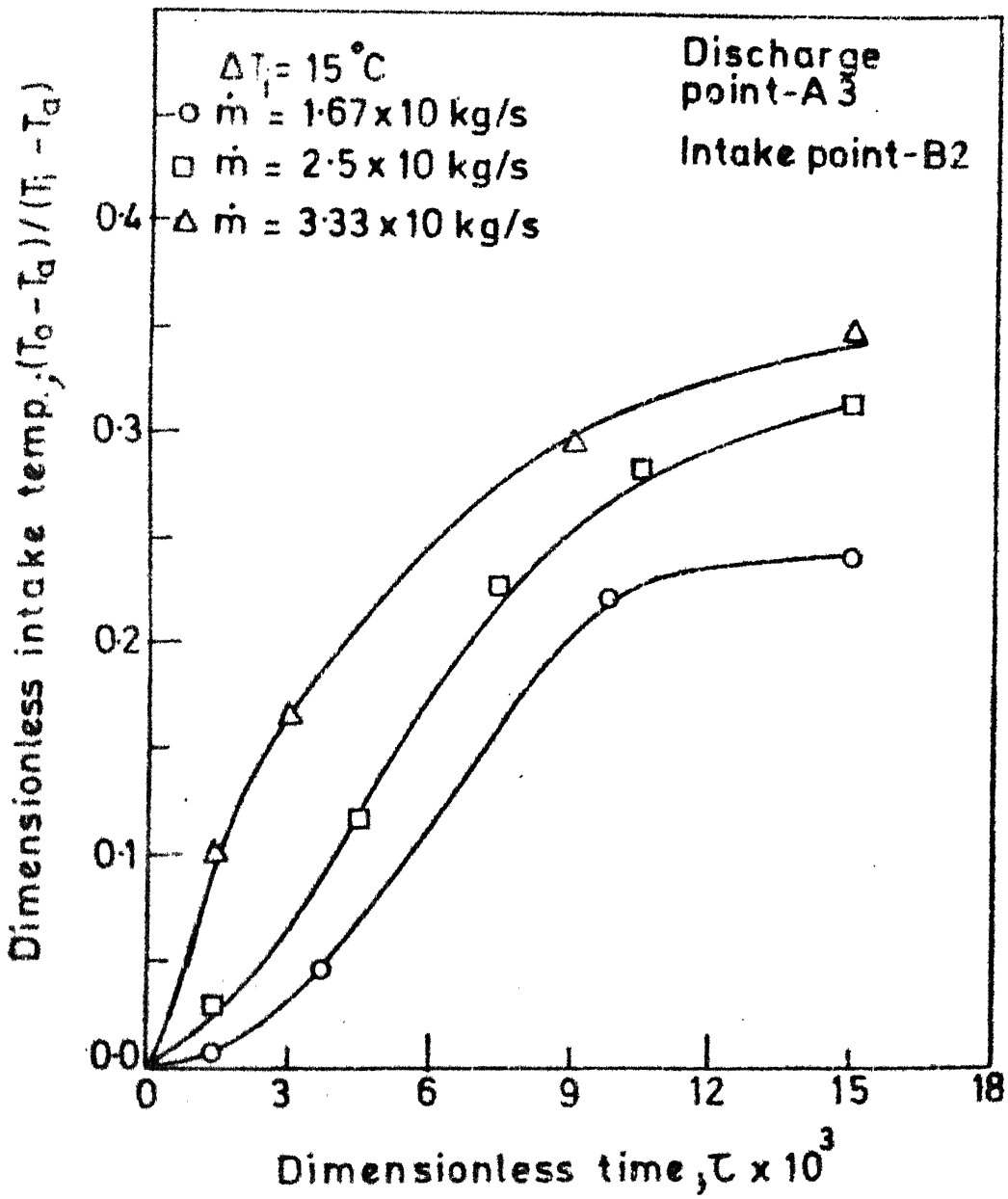

FIG·4·4 EFFECT OF INLET WATER FLOW RATE ON INTAKE TEMPERATURE.

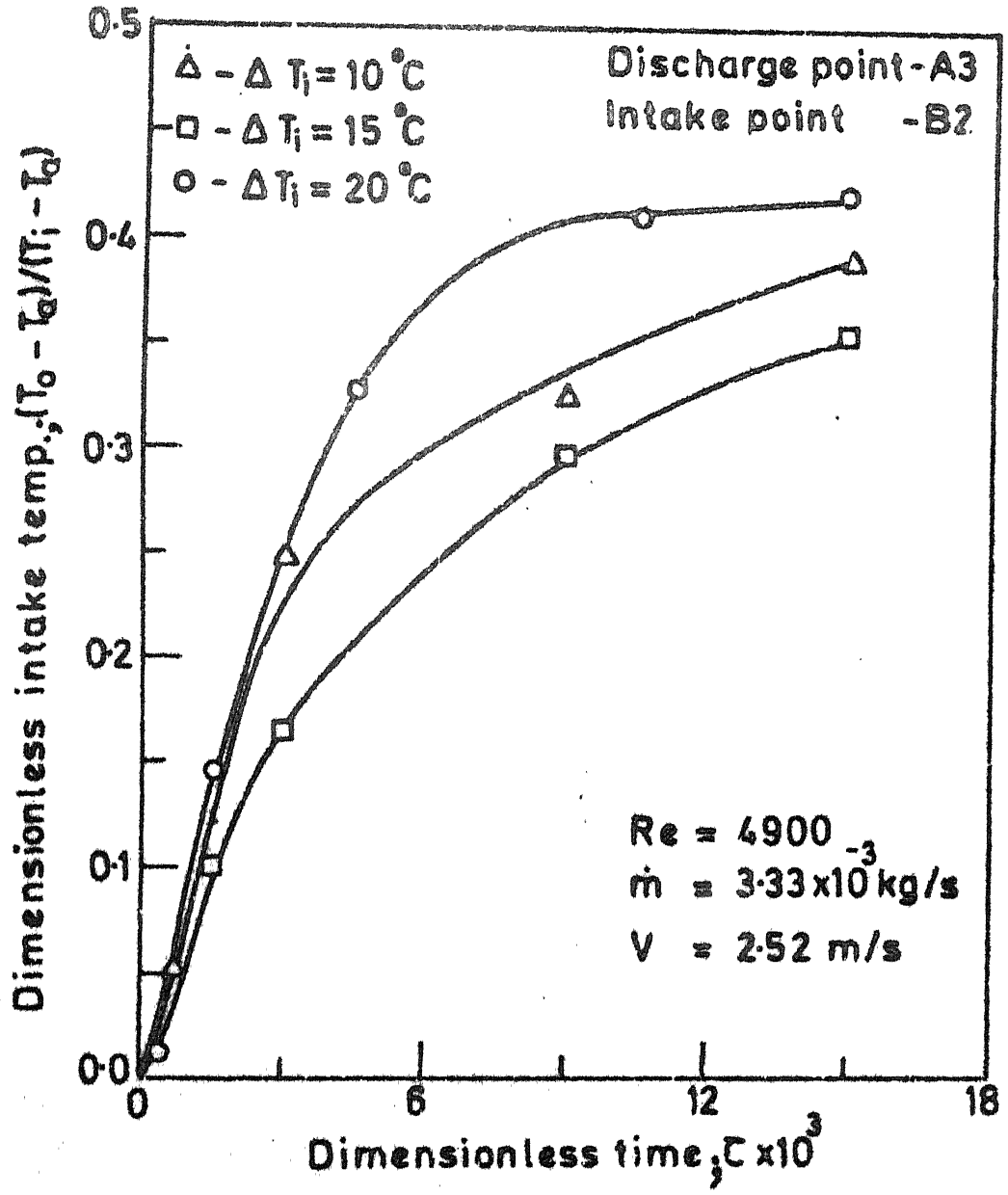

FIG·4·5 EFFECT OF INLET TEMPERATURE RISE ON INTAKE TEMPERATURE.

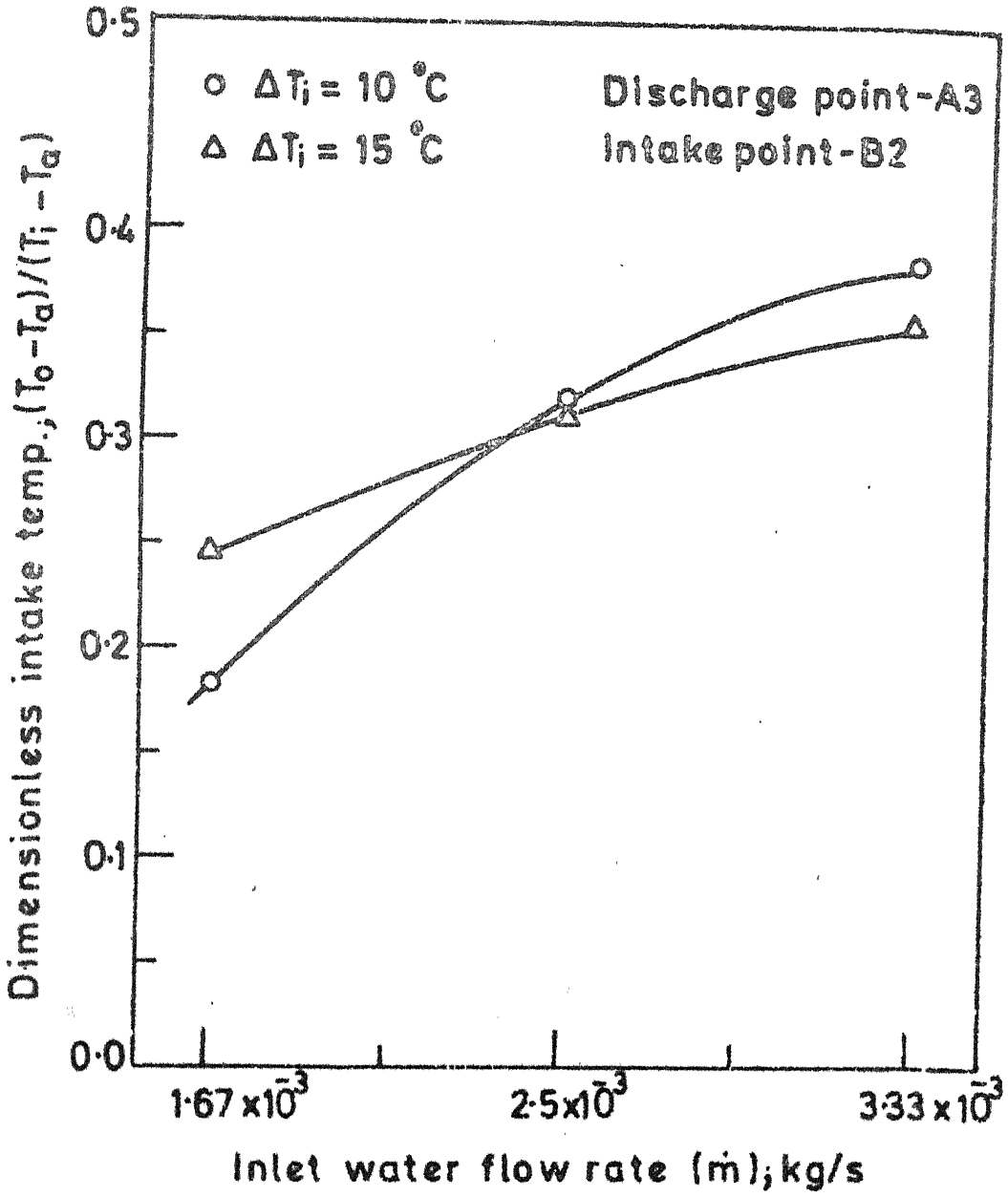

FIG. 4·6 VARIATION OF INTAKE TEMPERATURE WITH DISCHARGE CONDITIONS.

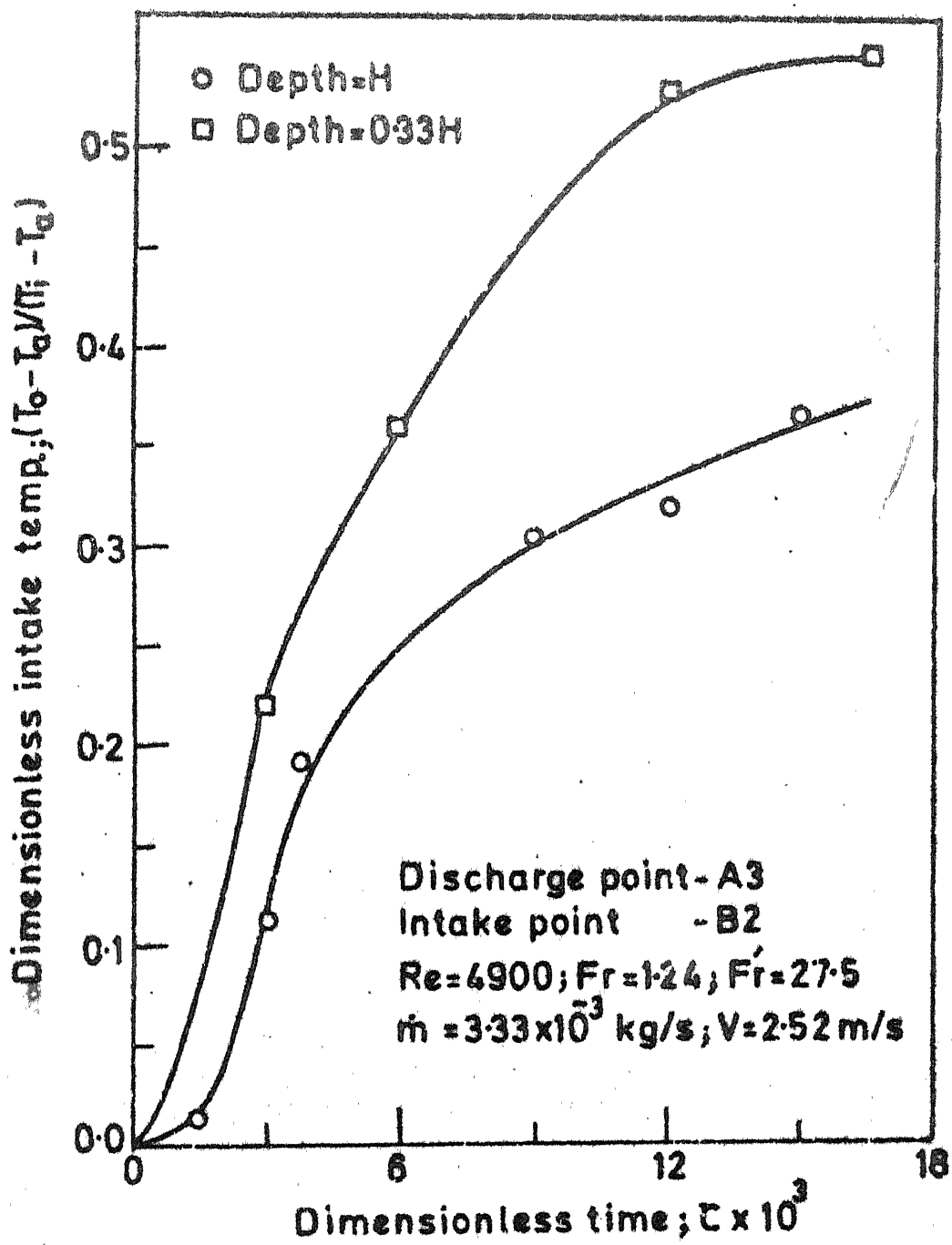

FIG·4·7 EFFECT OF POND DEPTH ON INTAKE TEMPERATURE.

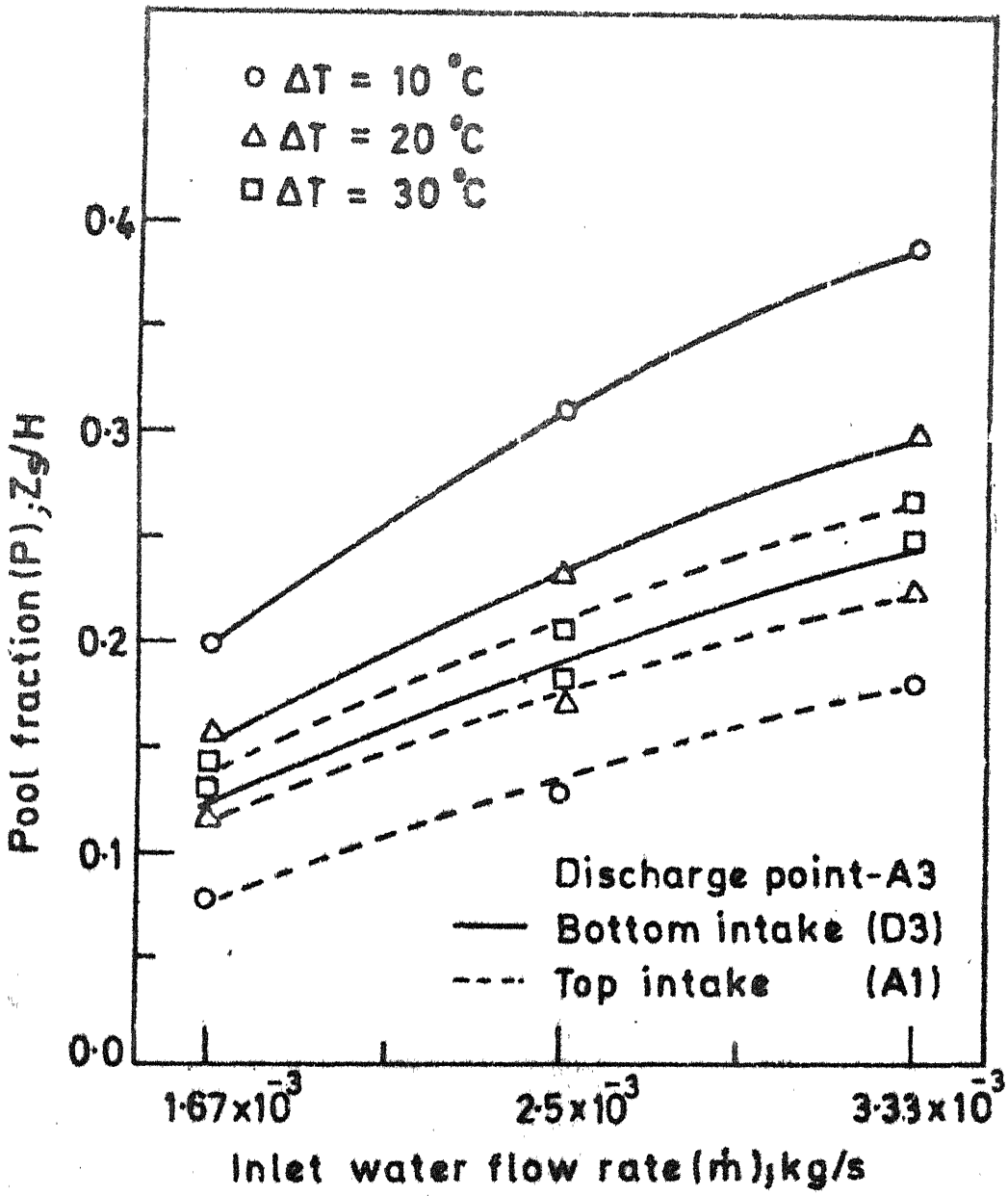

FIG·4·8 VARIATION OF POOL FRACTION WITH DISCHARGE CONDITIONS.

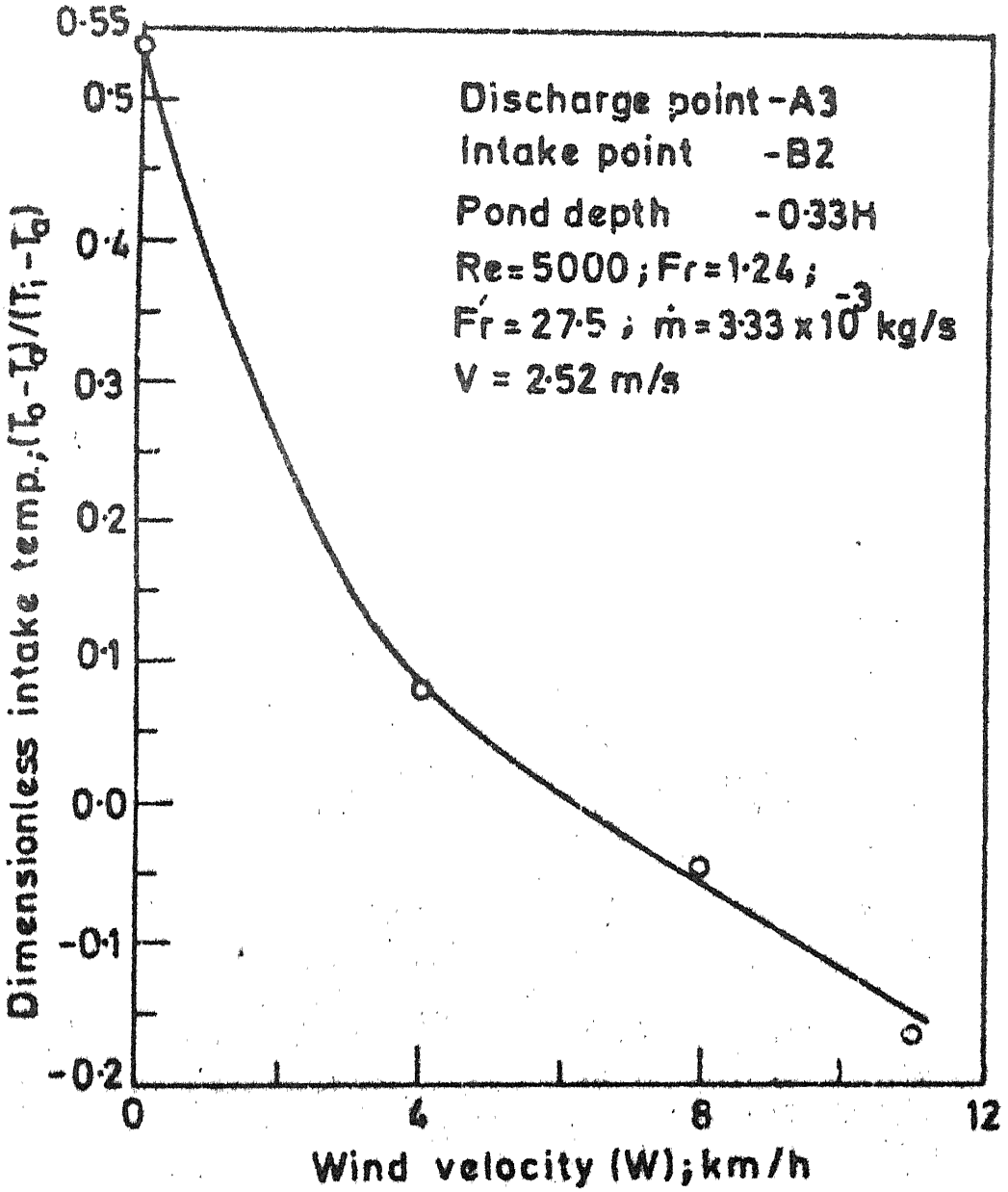

FIG. 4·9 EFFECT OF WIND VELOCITY ON INTAKE TEMPERATURE.

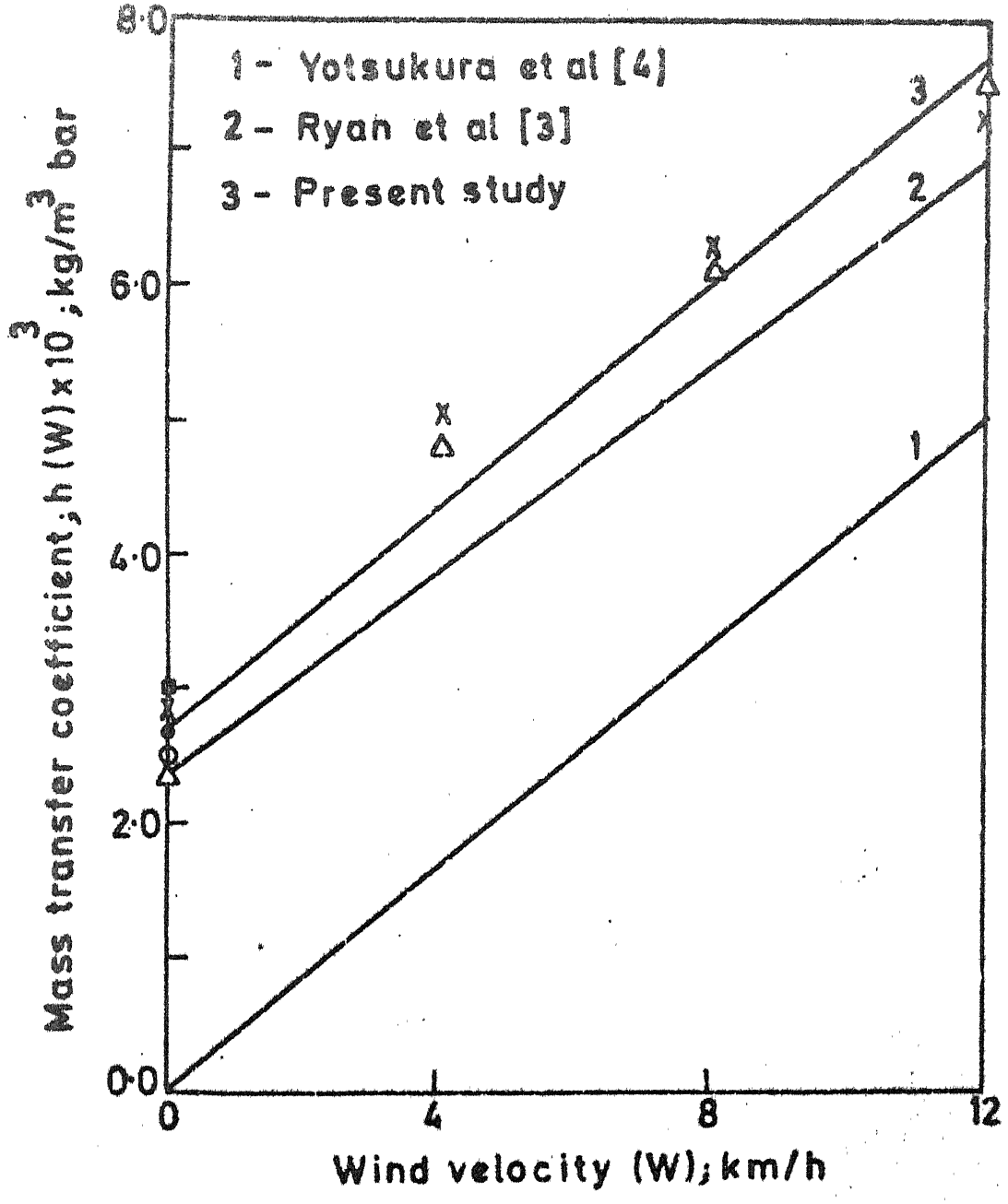

FIG.4·10 EFFECT OF WIND VELOCITY ON MASS TRANSFER COEFFICIENT

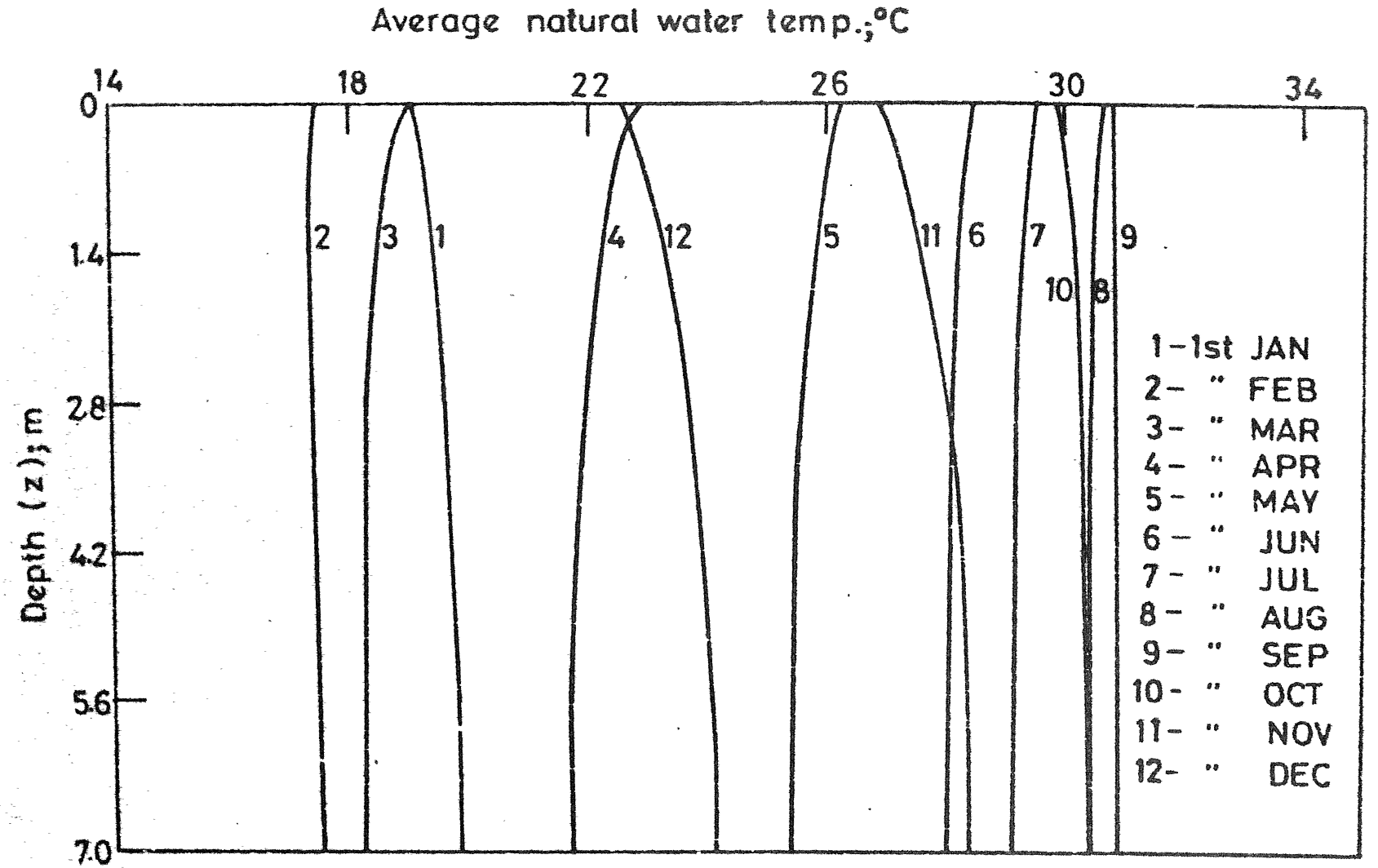

FIG. 4.1 NATURAL WATER TEMPERATURE VARIATION IN A WATER BODY.

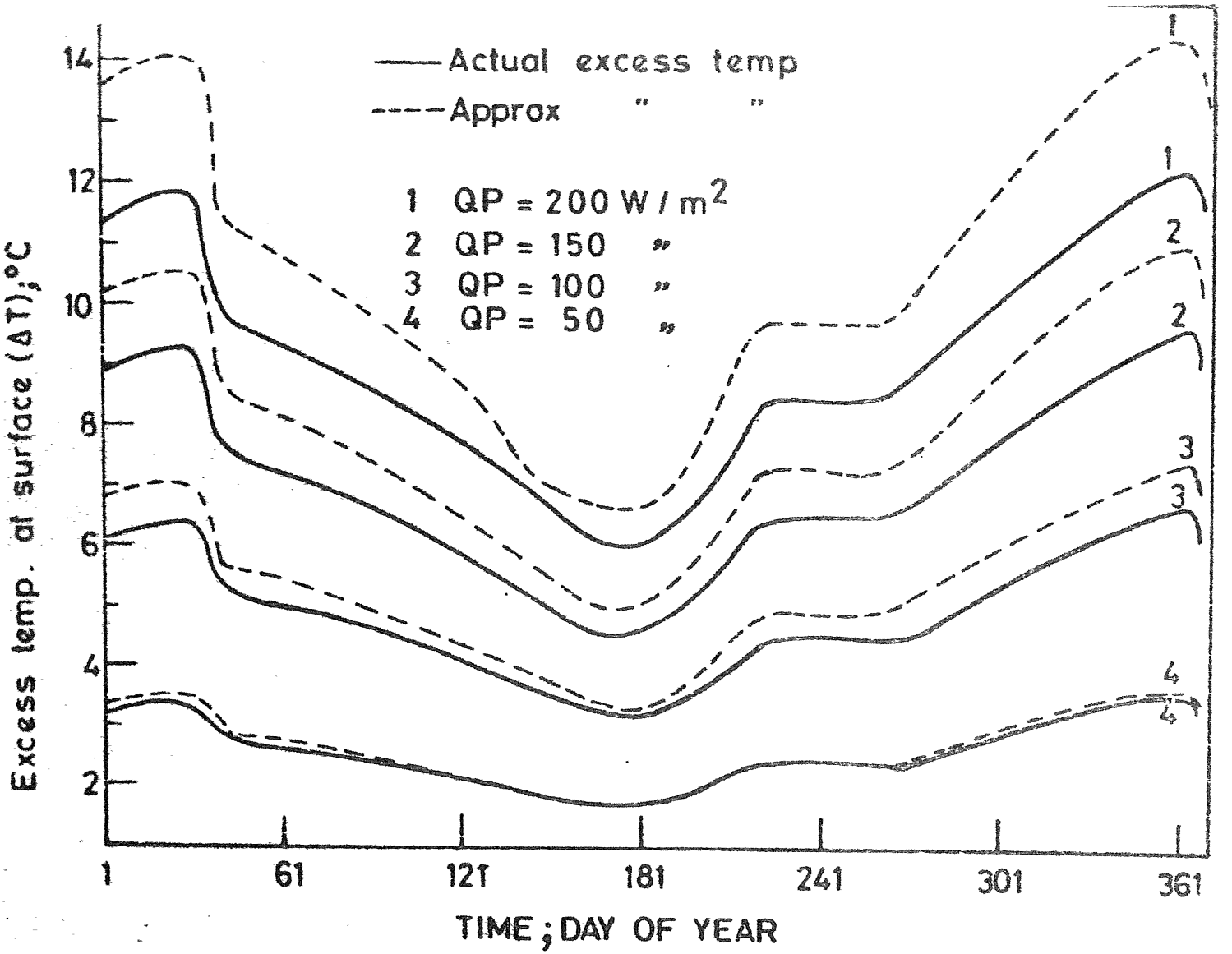

FIG.4-12 TRANSIENT VARIATION OF EXCESS TEMPERATURE AT SURFACE.

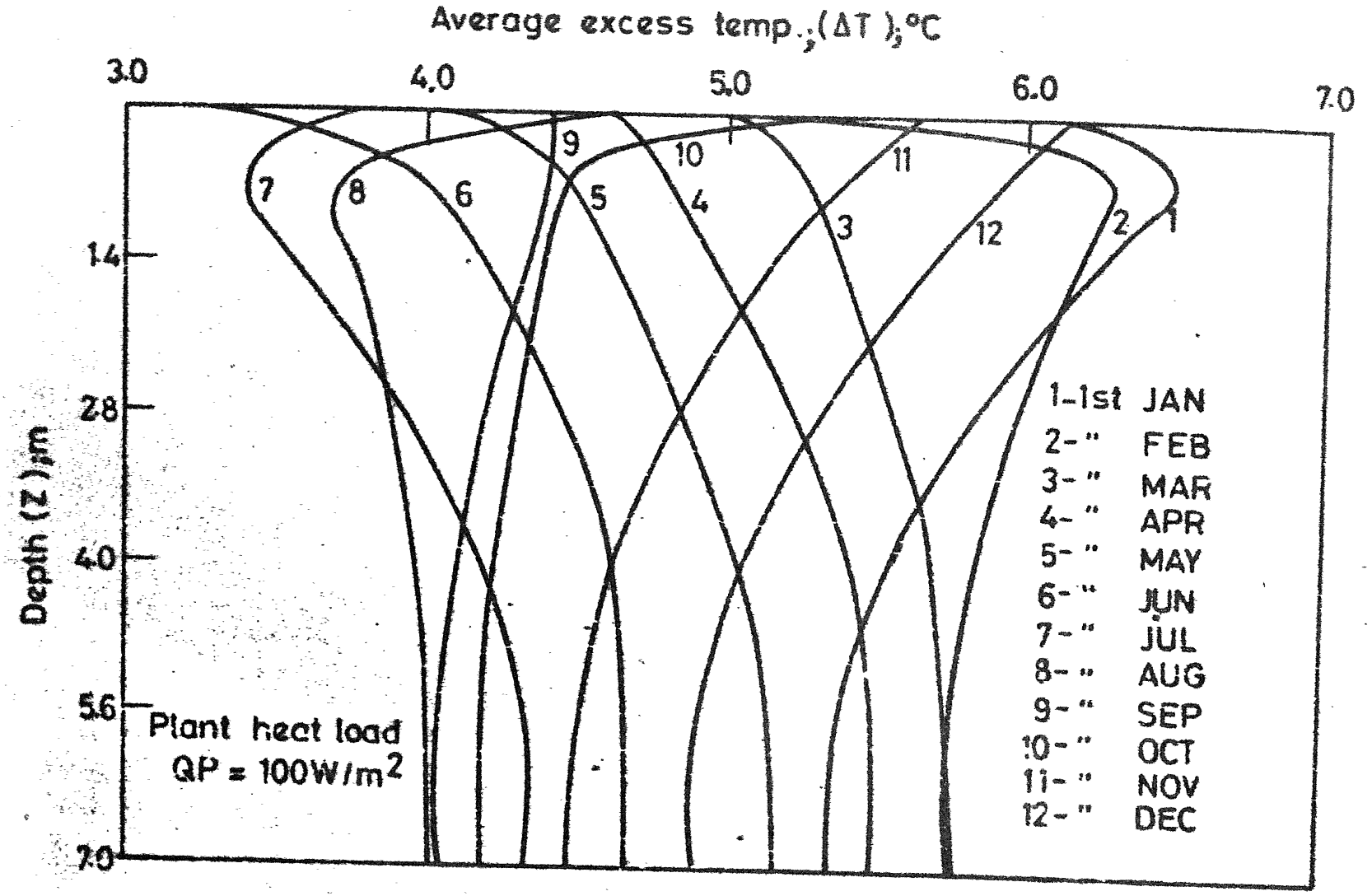

FIG. 4.13 EXCESS TEMPERATURE VARIATION IN A WATER BODY.

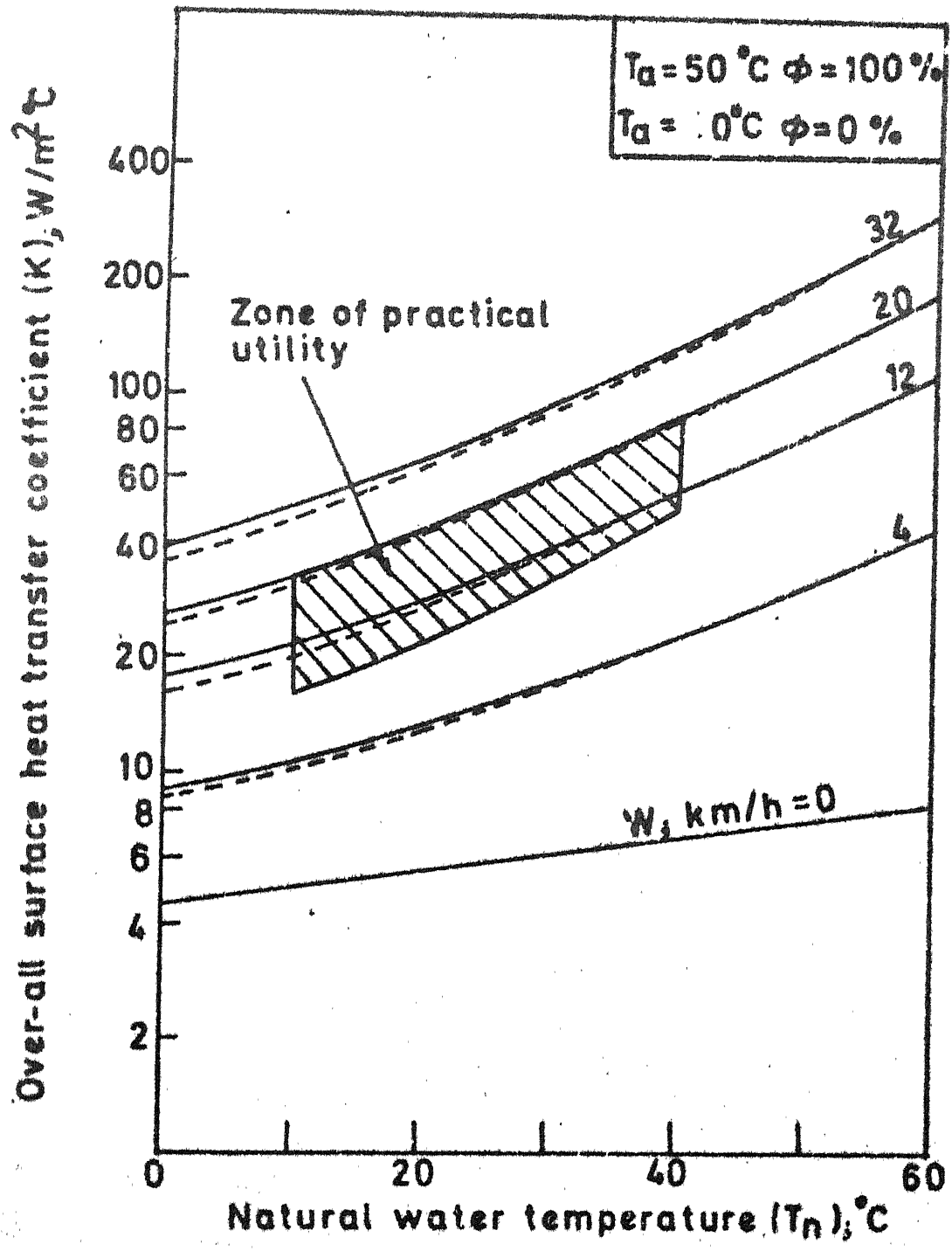

FIG. 4.14 EFFECT OF METEOROLOGICAL VARIABLES ON OVERALL SURFACE HEAT-TRANSFER COEFFICIE

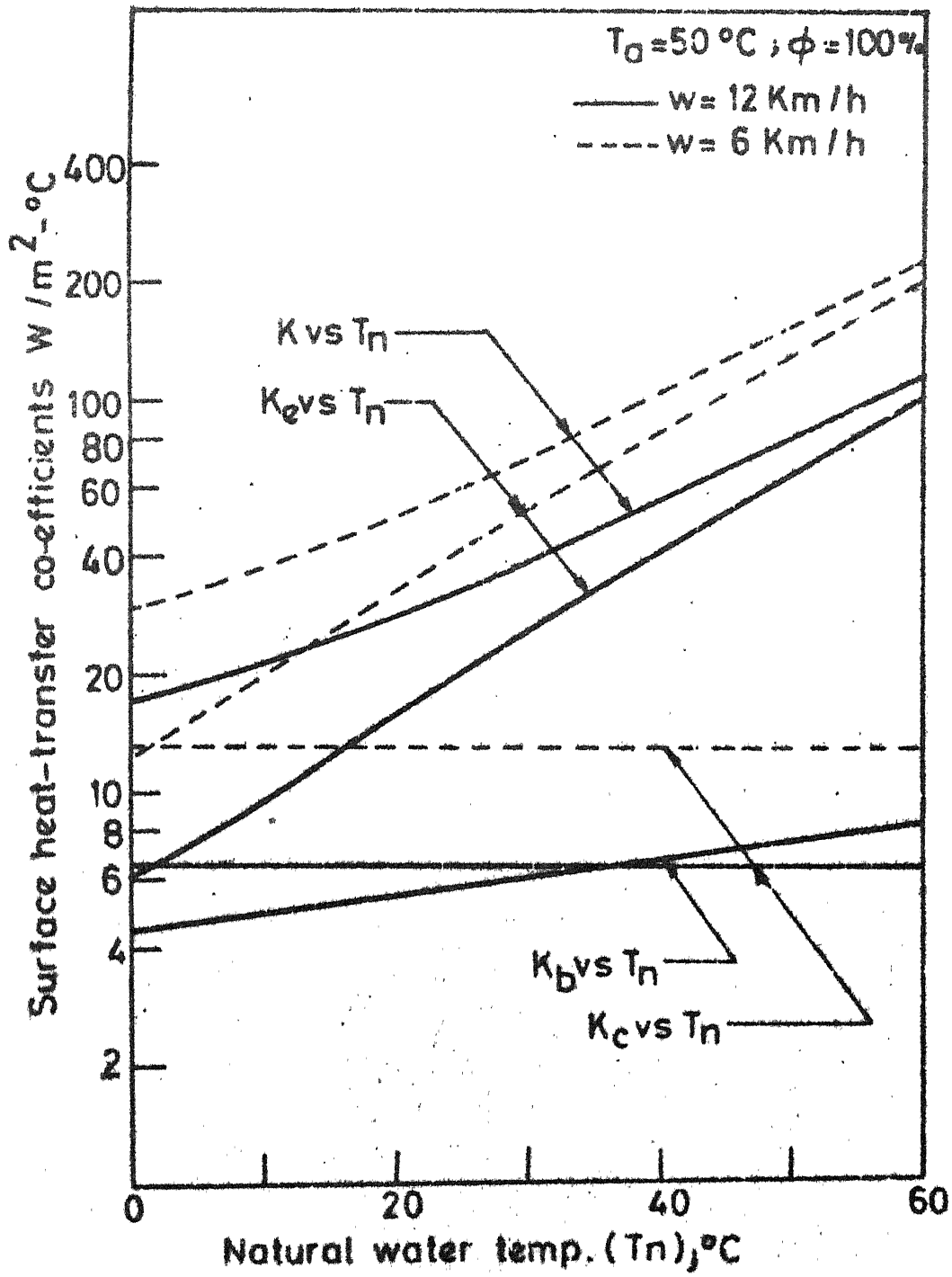

FIG.4.15 EFFECT OF METEOROLOGICAL VARIABLES ON SURFACE HEAT-TRANSFER COEFFICIENTS.

APPENDIX-I

Eq. 3.4.5 is written as

$$\frac{\partial T}{\partial t} = \varepsilon_Z \frac{\partial^2 T}{\partial Z^2} \qquad (A.1)$$

where

$$T = T_n - T_B$$

$$\frac{\partial T}{\partial t} = \frac{1}{\Delta t} (T_{i,j+1} - T_{i,j}) \qquad (A.2)$$

$$\frac{\partial^2 T}{\partial Z^2} = \frac{1}{\Delta H} (T_{i+1,j} - 2T_{i,j} + T_{i-1,j}) \qquad (A.3)$$

This gives

$$T_{i,j+1} = \frac{\Delta t \cdot \varepsilon_Z}{\Delta H^2} [T_{i+1,j} + T_{i-1,j}] + \left[1 - \frac{2\Delta t \cdot \varepsilon_Z}{\Delta H^2}\right] T_{i,j} \qquad (A.4)$$

Using $$M = \frac{\Delta H^2}{2\Delta t \cdot \varepsilon_Z} \qquad (A.5)$$

$$T_{i,j+1} = M [T_{i+1,j} + T_{i-1,j}] + [1 - M] T_{i,j}$$

.... (A.6)

Stability condition for A.6 require : $M \leq 1/2$

Finite difference representation of A.6 is :

$$T_{1,\ J+1} = M\ (T_{2,J} + T_{O,J}) + (1 - 2M)\ T_{1,J}$$

$$T_{2,\ J+1} = M\ (T_{3,J} + T_{1,J}) + (1 - 2M)\ T_{2,J}$$

$$\vdots \qquad \text{A.7}$$

$$T_{n,J+1} = M\ (T_{n+1,\ J} + T_{n-1,J}) + (1 - 2M)\ T_{n,J}$$

$$T_{n+1,J+1} = M\ (T_{n+2,J} + T_{n,J}) + (1 - 2M)\ T_{n+1,J}$$

Temperatures at fictitious points, $T_{O,J}$ and $T_{n+2,J}$ are obtained from the finite difference equations of the boundary conditions (Eqs. 3.4.6 and 7) which are:

$$(T_{2,J+1} - T_{O,J+1}) / 2\ \Delta H = - Q\ (T_{1,J},\ J.\Delta t)/\rho\ c_p\ \varepsilon_z \qquad \text{A.8}$$

and $$T_{n+2,J} - T_{n,J} = 0 \qquad \text{A.9}$$

Therefore, the finite difference representation of various elements in the water body is:

For $I = 1$: $$T_{I,J+1} = 2M[T_{I+1,J} + \Delta H\ \ Q(T_{I,J},\ J\ .\Delta t)/\rho\ c_p\ \varepsilon_z]$$

$$+ (1 - 2M)\ T_{I,J} \qquad \text{A.10}$$

$1 < I < n+1$: $$T_{I,J+1} = M[T_{I+1,J} + T_{I-1,J}]$$

$$+ (1 - 2M)\ T_{I,J} \qquad \text{A.11}$$

$I = n+1$: $$T_{I,J+1} = 2M\ \ T_{I-1,J} + (1 - 2M)\ T_{I,J} \qquad \text{A.12}$$

Similar difference equations are written for eq. (3.4.8) also.